From the Klinik für Gyäkologie und Geburtshilfe

(Director: Prof. Dr. med. Nicolai Maass)

at the University Medical Center Schleswig-Holstein, Campus Kiel

at Kiel University

Detection of copy number aberrations in endometrial cancer using array CGH

Inaugural dissertation

to acquire the doctoral degree (Dr. med.)

at the Faculty of Medicine

at Kiel University

presented by

Asiyan Nusilati

from Xinjiang, Volksrepublik China

Kiel 2023

1st Reviewer: Prof. Dr. rer. nat. Norbert Arnold

2nd Reviewer: Priv.-Doz. Dr. Eva Maria Murga Penas

Date of oral examination: 03.04.2024

Approved for printing, Kiel, 31.01.2024

Index

Abbreviations

AKT	Protein kinase B
APC	Adenomatous polyposis coli
ARID1A	AT-rich interactive domain-containing protein 1A
ARID5B	AT-rich interaction domain 5B
aCGH	Array comparative genomic hybridization
ATM	ATM Serine/Threonine Kinase
BAC	Bacterial artificial chromosome
BAP1	BRCA1 associated protein 1
BARD1	BRCA1 associated RING domain 1
BGN	Biglycan
BLM	Bloom syndrome RecQ like helicas
BMI	Body max index
bp	Base pairs
BRCA1/2	Breast cancer type 1 /2 susceptibility protein
BRIP1	BRCA1 interacting protein C-terminal helicase 1
cDNA	complementary DNA c
CGH	Comparative genomic hybridization
CHEK1/2	Checkpoint Kinase 1/2
CNNB1	Catenin beta 1
CNA	Copy number alteration
CNV	Copy number variation
DNA	Deoxyribonucleic acid
FANCA/C/D2/E/F/G/L	FA Complementation Group A/C/D2/E/F/G/L
FBXW7	F-Box and WD Repeat Domain Containing 7
FFPE	Formalin-fixed, paraffin-embedded
FGFR2	Fibroblast growth factor receptor 2

FIGO	International Federation of Gynecology and Obstetrics
FISH	Fluorescence in situ hybridization
gDNA	Genomic DNA
GSK-3β	Glycogen synthase kinase-3β
HNPCC	Hereditary nonpolyposis colorectal cancer
HR	Homologous recombination
KRAS	KRAS Proto-Oncogene, GTPase
LOH	Loss of heterozygosity
LST	Large-scale state transitions
LVSI	Lymph-vascular space invasion
MLH1	MutL Homolog1
MMR	DNA mismatch repair
MRE11A	MRE11 Homolog, double strand break repair nuclease
MSH2	MutS homolog2
MSH6	MutS homolog6
MSI	Microsatellite instable
MSS	Microsatellite stable
mTOR	The mammalian target of rapamycin
NBN	Nijmegen breakage syndrome 1 (Nibrin)
NGS	Next generation sequencing
OGT	Oxford Gene Technology
PALB2	Partner and localizer of BRCA2
PARP	poly (ADP-ribose) polymerase
PBS	Phosphate buffered saline
PCOS	Polycystic ovarian syndrome
PCR	Polymerase chain reaction
PD-1	Programmed cell death protein 1
PD-L1	Programmed death-ligand 1

PMS2	Postmeiotic segregation increased 2
PIK3CA	Phosphatidylinositol-4,5-Bisphosphate3-Kinase Catalytic Subunit Alpha
PIK3R1	Phosphoinositide-3-Kinase Regulatory Subunit 1
PI3K	Phosphatidylinositol3-kinase
POLE	DNA polymerase epsilon
POLEEDM	POLE exonuclease domain mutations
PORTEC	Post-operative radiation therapy endometrial cancer
ProMisE	Proactive Molecular Risk Classifier for Endometrial Cancer
PTEN	Phosphatase and tensin homolog
QC	Quality control
RAD50	RAD50 double strand break repair protein
RAD51	DNA repair protein RAD51 recombinase
RAD51B	RAD51 Paralog B
SMGs	Significantly mutated genes
SNP	Single nucleotide polymorphism
TAI	Telomeric allelic imbalance
TCGA	The Cancer Genome Atlas
TNM	Tumor Node Metastasis
TP53	Tumor protein 53
UICC	Union for International Cancer Control
WHO	World Health Organisation
WRN	Werner syndrome ATP-dependent helicase
ZFHX3	Zinc finger homeobox 3

1 Introduction

Cancer is a disease of uncontrollably abnormal cell growth with the potential to invade to neighbor organs as well as spread to distant organs. The genes that regulate cell growth and cell differentiation must be altered to initiate the carcinogenic process in the development of normal cell into a cancer cell (Croce 2008). The genetic alterations in somatic cells can occur on different levels and by different mechanisms. For example, gain or loss of a section of a certain chromosome, or gene mutations which are variations in the nucleotide sequence of a genomic DNA could cause cancer. For an effective cancer treatment an early and accurate diagnosis is essential. Early diagnosis improved cancer outcomes by providing individualized therapy at the earliest possible stage. Consequently, it reduces mortality and improves the quality of life. Cytogenetic along with molecular biology techniques are a valuable tool in the field of cancer research and cancer treatment due to their great potential in early diagnosis and targeted therapeutic agents. In the last decade, many experimental and computational approaches have been developed to discover genomic variants. Among them array comparative genomic hybridization (aCGH) as one of the methods designed to detect segmental genomic alterations by identifying copy number variations (CNVs), has become an important tool in cancer research and cancer diagnosis.

1.1. Gynecological malignancies

Most common gynecological cancers include uterine, cervical and ovarian malignancies. Similar to other types of cancers, gynecological malignancies are complex diseases driven by different factors, including genetic and epigenetic alterations. Therefore, clarification of the molecular and genetic mechanisms of development or progression of gynecological cancers are critical for discovery of new targets for both diagnosis and treatment of the patients. This thesis will focus on endometrial cancer, which is one of the most common malignancies of gynecological cancers. Endometrium is the innermost lining layer of the uterus. Over the whole fertile years of a women's life, it is subject to a process of cyclical change. The majority of cancers that occur in the body of uterus are endometrial cancers, which arise from the epithelial lining of the uterine cavity (Amant et al. 2018).

1.1.1. Epidemiology

Endometrial cancer is the most common gynecological malignancy in developed countries and its incidence is increasing (Morice et al. 2016). The recent report from the National Cancer Institute estimated the age-adjusted endometrial cancer incidence rate (new cases per 100,000 person years) in the Unites States is 27.8/ 100,000 and rates for new cases have been rising on average 0.8% each year over 2008–2017 (National Cancer Institute). In 2020, according to an estimate, there will be

65,620 new endometrial cancer cases diagnosed in the Unites States (Siegel et al. 2020). In Europe, the endometrial cancer is reported to be the fourth most frequent cancer type in women. In 2020, the estimated age-standardized incidence rates are 28.9/100,000 in Europe and 24.8/100,000 in Germany (Figure 1) (European Cancer Information System 2020). 11,200 new cases are estimated to be diagnosed in Germany in 2020 (Robert-Koch-Institut). Overall, the prognosis of endometrial cancer is good with 5-year relative survival rates 81 % (National Cancer Institute). Endometrial cancer is the 9th cause of cancer death for women in Europe, with an estimated mortality rate of 6.2/100,000 (European Cancer Information System 2020). Although at the moment of diagnosis the majority of women of endometrial cancer have early-stage disease and a good long-term prognosis, about 13 % of those patients end up relapsing and have the mortality rate around 25 % (Fung-Kee-Fung et al. 2006).

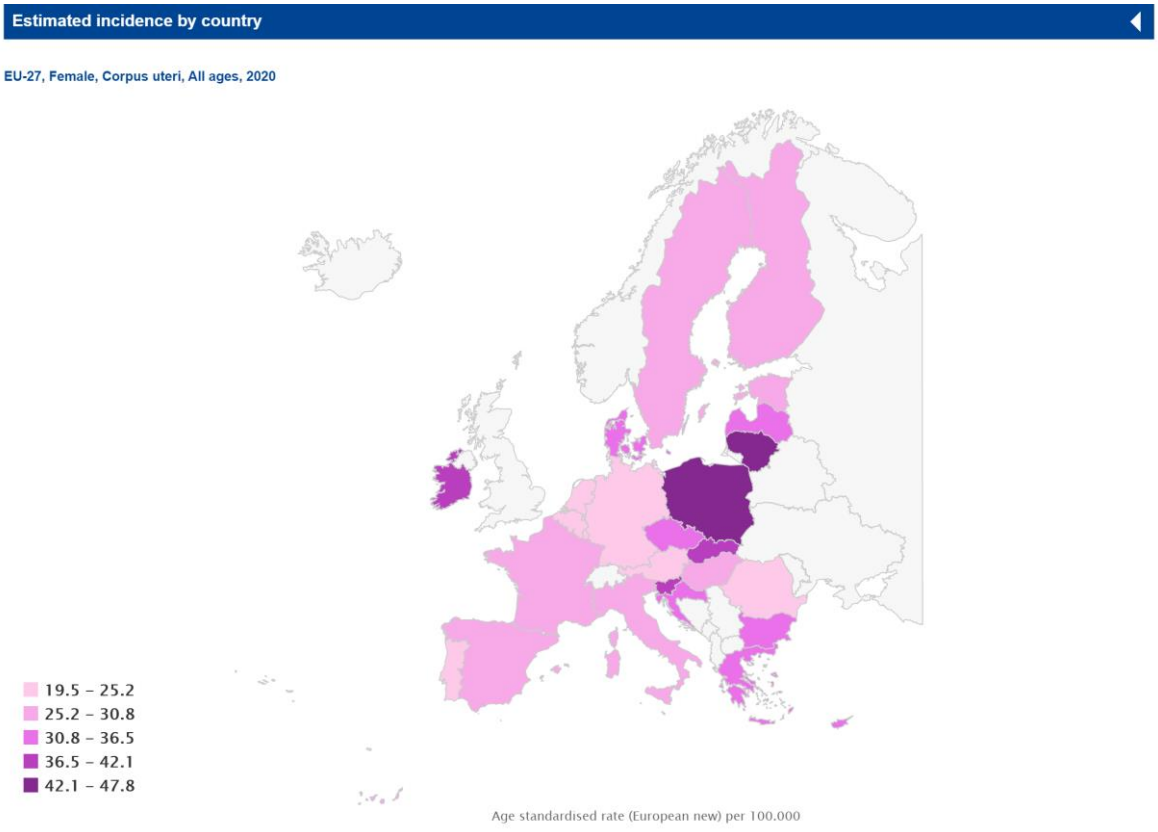

Figure 1: Estimated age-standardized incidence rate of corpus uteri cancer per 100,000 person-years in EU 2020 (European Cancer Information System 2020, https://ecis.jrc.ec.europa.eu/).

In cancer incidence and mortality registries, endometrial cancers are recorded within the cancer of uterine corpus, the latter also include uterine sarcomas. Uterine sarcomas are rare tumors that account for less than 5 % of all uterine malignancies and incidence rate is 1.5-3/100,000 (Sherman and Devesa 2003; Denschlag et al. 2019), supporting that the observed incidence of uterine corpus cancer mainly reflects the increased incidence of endometrial cancer.

1.1.2. Etiology and Risk factors

Approximately 90 % of endometrial cancers are sporadic, and the remaining 10 % are hereditary (Okuda et al. 2010). Bokhman categorized endometrial cancer into two pathogenetic types using both clinical and histopathological variables: estrogen-dependent endometrioid endometrial cancer or type

I, and non-endometrioid endometrial cancer, or type II tumors (Bokhman 1983). Many factors affect the risk of developing endometrial cancer. The risk of endometrial cancer increases with age, more than 90 % of cases of endometrial cancer occur in women older than 50 years of age (Colombo et al. 2016). In Germany, women older than 70 years of age have highest incidence rate of getting endometrial cancer (Figure 2).

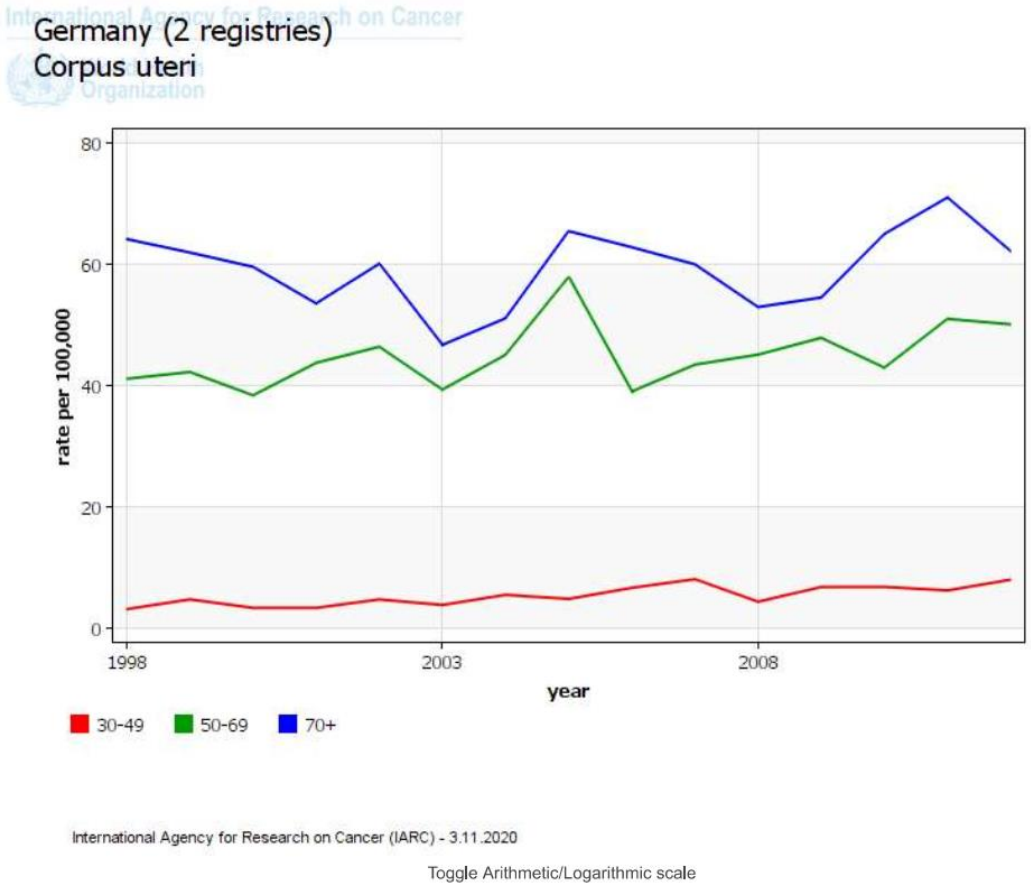

Figure 2: Trends in the incidence of corpus uteri cancer by age group in Germany (International Agency for Research on Cancer, https://ci5.iarc.fr/)

Another established risk factor for the development of endometrial cancer is obesity. Women with body mass index (BMI) greater than 25 kg/m^2 have an increased risk of getting endometrial cancer (Bianchini et al. 2002). A recent study by Shaw et.al (Shaw et al. 2016) showed that obesity (defined as BMI > 30 kg/m^2 and < 35 kg/m^2) was associated with a 2.6-fold increase in endometrial cancer risk, while severe obesity (BMI > 35 kg/m^2) was associated with a 4.7-fold increase in endometrial cancer risk compared to normal-weight women (BMI < 25 kg/m^2). Overweight women have more risk developing an endometrial cancer. The reasons for this can be the increased production of estrogen in adipocytes (Zhang et al. 2012b), or the increased chance of producing cancer cells due to insulin resistance (Shao et al. 2016). Diabetes mellitus also increase the risk of endometrial cancer in women. The prospective study from Frieberg et al. established that diabetes was associated with a 2-fold

increased risk for endometrial cancer, and combination of diabetes with obesity and low physical activity was associated with a further increased risk for endometrial cancer (Friberg et al. 2007).

Tamoxifen, a nonsteroidal antiestrogen agent, is normally used for the treatment of both early and advance estrogen receptor-positive breast cancers. Simultaneously, tamoxifen can increase the risk of endometrial cancer, as it is thought to have a similar effect as estrogen on the endometrial. Risk of endometrial cancer increased with longer duration of tamoxifen use. The tamoxifen-induced endometrial cancers often belong to less favorable subtypes and have relatively poor prognoses (Jones et al. 2012). In addition, postmenopausal women who use hormone replacement therapy containing estrogen or tibolone alone, without gestagen protection are at increased risk of endometrial cancer (Beral et al. 2005).

Polycystic ovarian syndrome (PCOS) is also well established as a risk factor for endometrial cancer. In women with PCOS younger than 54 years old, the risk of developing endometrial cancer is 3.8-fold higher than premenopausal women (Barry et al. 2014). Additionally, increased risk is associated with early age at menarche, late menopause, nulliparity, irregular menstruation and family history of endometrial cancer (Haidopoulos et al. 2010).

Endometrial cancer can also be a part of hereditary Lynch syndrome, which is also called hereditary nonpolyposis colorectal cancer (HNPCC). HNPCC is caused by mutations in DNA mismatch repair (MMR) genes (*MLH1*, *MSH2*, *PMS2*, or *MSH6*), which is a hereditary predisposition to many tumors, in the forefront of which endometrial cancer in women. The age at diagnosis of HNPCC associated endometrial cancer is approximately 2 decades younger than that for sporadic endometrial cancers (Marra and Boland 1995). Cumulative risk for HNPCC of developing endometrial cancer by age 70 years for women are approximately 42 % to 60 % (Aarnio et al. 1999; Win et al. 2012).

1.1.3. Pathogenesis and histological or molecular classifications

1.1.3.1. Histopathology

Endometrial cancer is characterized by neoplasia of the glandular tissue of the endometrium and is subdivided into type I and type II based on histologic properties, hormone receptor expression and grade (Table 1.1). Type I, due to its histological similarity to the endometrium, is also called the endometrioid type, which is primarily a low-grade endometrioid hormone receptor-positive tumor and arises on the basis of endometrial hyperplasia. Type I occurs in obese women afflicted by hyperlipidemia / diabetes and it is caused by hyperestrogenism. Type II endometrial cancer is also described as non-endometroid and it is associated with atrophic endometrium. It is hormone - receptor-negative tumor and occurs more common in non-obese women. Type II endometrial cancer is high grade tumor which is clinically aggressive and has tendency to metastases. Normally it is

diagnosed in the advanced stages of the disease and has unfavorable prognosis (Bokhman 1983; Creasman et al. 2003; Hamilton et al. 2006; Wilczyński et al. 2016).

Table 1.1: Characteristic of type I and type II endometrial cancer.

	type I	**type II**
grade	low	high
hormone receptor expression	positive	negative
tumor grade	low (grade1-2)	high (grade3)
histology	endometroid	non-endometroid (serous, clear cell)
background endometrium	hyperplasia	atrophy
obesity	yes	no
prognosis	good	poor
genetic factors	*PTEN*, *KRAS* and *CTNNB1* mutations, MSI	*TP53* mutation

Histologically, epithelial carcinoma comprises endometrioid, high grade serous, clear cell, mucinous, squamous cell, transitional cell, small cell and undifferentiated, mixed carcinoma (two of above histological types in which minor component accounts for 10 % or more of the tumor) (Tavassoli and Devilee 2003). Endometrioid, serous and clear cell carcinoma account for 75 %, 5-10 %, and 1-5 % respectively (Murali et al. 2014; Tavassoli and Devilee 2003).

Histopathologic grades of endometrial cancer according to International Federation of Gynecology and Obstetrics (FIGO) classification. FIGO grade is based on the degree of glandular differentiation, which are grouped as follows (Table 1.2) (Amant et al. 2018).

Table 1.2: FIGO histopathologic grade classification of endometrial cancer.

G1	< 5 %	nonsquamous or nonmorular solid growth pattern
G2	≥ 5 – 50 %	nonsquamous or nonmorular solid growth pattern
G3	> 50 %	nonsquamous or nonmorular solid growth pattern

1.1.3.2. Molecular classification

The Cancer Genome Atlas (TCGA) has provided a comprehensive genomic and transcriptomic analysis of 373 endometrial cancer and described the molecular process of these tumors in detail, which allowed them to stratify endometrial cancer into four distinct molecular subtypes: ultra-mutated/

POLE-mutant, microsatellite instable (MSI)/ hypermutated, microsatellite stable (MSS)/ copy number low, and serous-like/ copy number high(Table 1.3) (Kandoth et al. 2013).

Ultra-mutated/ *POLE*-mutant group includes approximately 10 % of endometrial cancers with significantly better prognosis compared to other subtypes. It consists of a stable somatic copy number alterations (CNAs) but highly mutant genes, in particular *POLE*. *POLE* is a catalytic subunit of DNA polymerase epsilon involved in nuclear DNA replication and repair. Significantly mutated genes (SMGs) which contribute to classification of this group included *POLE* (100 %), *PTEN* (94 %), *BRCA2* (77 %), *APC* (88 %), *PIK3CA* (71 %), *PIK3R1* (65 %), *FBXW7* (82 %), *ARID1A* (76 %), *KRAS* (53 %) and *ARID5B* (47 %) (Kandoth et al. 2013).

MSI/ hypermutated subtype is characterized by a high mutation rate and a microsatellite instability phenotype that is indicative of defective mismatch repair resulting from *MLH1* silencing (Hong et al. 2015; Park et al. 2013). In addition, it consists mainly endometrioid type with less favorable prognosis (Kandoth et al. 2013).

MSS/copy number low group is classified by genomic stability and microsatellite stability. It has lower mutation rate and mostly belongs to endometroid type. The difference from the MSI group depends on 100 % mutation in chromosome1q and 52 % mutation in *CNNB1*. Compared with MSI subtype, it has a better prognosis (Kandoth et al. 2013).

The fourth subgroup is serous-like/copy number high group, it is genomically unstable and almost all *TP53* mutant. This type comprises mainly serous endometrioid cancer and 19 % grade 3 endometroid cancer. Unsurprisingly, the prognosis is worse than the other 3 clusters. (Hong et al. 2015; Kandoth et al. 2013; Cosgrove et al. 2018).

Table 1.3: TCGA molecular classification of endometrial cancer.

	ultra-mutated/ *POLE*-mutant	**MSI/ hypermutated**	**MSS/copy number low**	**serous-like/copy number high**
CNAs	low	low	low	high
mutation rate	very high	high	low	low
commonly mutated genes	*POLE* (100 %) *PTEN* (94 %) *CCNB3* (94 %) *APOB* (94 %) *CSMD3* (94 %) *ABCA5* (88 %) *APC* (88 %) *FBXW7* (82 %) *ZFHX3* (82 %) *BRCA2* (77 %) *ARID1A* (76 %) *PIK3CA* (71 %) *KRAS* (53 %) *ARID5B* (47%) *TP53* (35%) *RPL22* (29%)	*PTEN* (88 %) *PIK3CA* (54 %) *ARID1A* (37 %) *RPL22* (37 %) *AR1D5B* (23 %) *KRAS* (35 %) *ZFHX3* (31 %) *CTNNB1* (20 %) *FGFR2* (14 %) *FBXW7* (11 %)	*PTEN* (77 %) *PIK3CA* (53 %) *CTNNB1* (52 %) *ARID1A* (42 %) *KRAS* (16 %) *FGFR2* (13 %) *CHD4* (12 %) *SPOP* (10 %) *CSMD3* (10 %) *FBXW7* (6 %)	*TP53* (92 %) *PIK3CA* (47 %) *FBXW7* (22 %) *PPP2R1A* (22 %) *CHD4* (13 %) *PTEN* (10 %) *CSMD3* (10 %)
microsatellite status	microsatellite variable	MSI	MSS	MSS
tumor grade	grade 1-3	grade 1-3	grade 1-2	grade 1-3
histology	endometrioid	endometrioid	endometrioid	serous, endometroid and serous mixed, endometroid
prognosis	good	medium	medium	poor

1.1.4. Classification systems for stage of disease at diagnosis

The stage is one of the most important factors in deciding the adequate treatment and in determining the successful rate. The staging system should not be changed after biopsy or initial treatment has been determined, the subsequent course of the disease does not affect the initial extent of the disease. There are two main systems used for staging endometrial cancer, the FIGO system and the Union for International Cancer Control (UICC) Tumor Node Metastasis (TNM) staging system.

1.1.4.1. FIGO staging

FIGO staging classification system is unique to gynecological tumors. The staging guidelines apply to all histological subtypes of endometrial cancer (Table 1.4). Rules for classification include histologic verification of grading and extent of the tumor (Amant et al. 2018).

1.1.4.2. TNM staging

Endometrial cancer can also be staged using the TNM system. This system codes the extent of the primary tumor (T), regional lymph nodes (N), and distant metastases (M) and provides a “stage grouping” based on T, N, and M. Individual TNM values can be combined to create a grouped variable representing stages I-IV, which are compatible with FIGO stage I-IV (Edge and Compton 2010).

Table 1.4: FIGO staging compared with the TNM classification (Amant et al. 2018).

FIGO stage	Union for International Cancer Control (UICC)			description
	T (tumor)	N[a] (lymph nodes)	M[b] (metastasis)	
I	T1	N0	M0	tumor confined to the corpus uteri
IA	T1a	N0	M0	no or less than half myometrial invasion
IB	T1b	N0	M0	invasion equal to or more than half of the myometrium
II	T2	N0	M0	tumor invades cervical stroma, but does not extend beyond the uterus
III	T3	N0-N1	M0	local and/or regional spread of the tumor
IIIA	T3a	N0	M0	tumor invades the serosa of the corpus uteri and/or adnexae
IIIB	T3b	N0	M0	vaginal involvement and/or parametrial involvement
IIIC1	T1-T3	N1	M0	metastases to pelvic lymph nodes
IIIC2	T1-T3	N1	M0	metastases to para-aortic nodes with or without positive pelvic lymph nodes
IVA	T4	Any N	M0	tumor invades bladder and/or bowel mucosa
IVB	Any T	Any N	M1	distant metastasis, including intra-abdominal metastases and/or inguinal nodes

1.1.5. Endometrial cancer management

1.1.5.1. Surgical treatment

Endometrial cancer is usually treated primarily by surgery, and surgical staging has become part of the initial management of endometrial cancer for both the prognostic stratification and determine of whether patients may benefit from chemotherapy or radiation therapy.

Surgery includes a total hysterectomy and bilateral salpingo-oophorectomy. The standard operation for women with advanced-stage endometrial cancer consists of removal of the uterus, ovaries, and tubes, pelvic and para-aortic lymphadenectomy, and if possible, resection of all visible tumor. Omentectomy is usually included for clear cell and serous cancer. Conventional oncologic surgery for endometrial cancer is performed by laparotomy, but nowadays the medical and technological advances allow the performance of the surgery through minimally invasive techniques such as laparoscopic surgery or robot-assisted laparoscopic surgery (Ghazali et al. 2019; Salehi et al. 2017).

1.1.5.2. Adjuvant treatment

No adjuvant treatment is indicated for patients with low-risk endometrial cancer (stage I endometrioid, grade 1–2, <50 % myometrial invasion, lymph-vascular space invasion (LVSI) negative) (ASTEC/EN.5 Study Group 2009; Sorbe et al. 2009). For patients with intermediate-risk endometrial cancer (stage I endometrioid, grade 1–2, ≥50 % myometrial invasion, LVSI negative), adjuvant brachytherapy is recommended to reduce vaginal recurrence. Patients with grade 1-2 tumors with deep (≥50 %) myometrial invasion and unequivocally positive (substantial, not focal) LVSI, and those with grade 3 tumors with <50 % myometrial invasion regardless of LVSI status, are referred to as high-intermediate-risk in the current classification. For these patients, brachytherapy or external beam radiotherapy is recommended as adjuvant therapy. External beam pelvic radiotherapy is the standard therapy for high-risk endometrial cancer (stage I endometrioid, grade 3, ≥50 % myometrial invasion, regardless of LVSI status) and is indicated to maximize pelvic control. Sequential adjuvant chemotherapy may be considered to improve progression free survival and cancer specific survival (Colombo et al. 2016).

1.1.5.3. Fertility-preserving therapy

Young patients who are still planning to have children and wish to have fertility preservation and have been established a diagnosis of a well-differentiated (G1) type I endometrial cancer expressing progesterone receptors, the uterus and adnexa may be left in place. Most commonly used conservative medical treatments are medroxyprogesterone acetate or megestrol acetate or a levonorgestrel intrauterine device. If complete remission of the endometrial cancer is observed after 6 months of treatment, the planned pregnancy should be attempted, if necessary, in collaboration with a reproductive medicine specialist. Hysterectomy should be carried out when the cancer does not respond after 6 months of conservative treatment. When the patient is not currently wishing to have a child, maintenance therapy and endometrial biopsy should be done every 6 months. Total hysterectomy and bilateral salpingo-oophorectomy should be recommended once the patient has had children or no longer wishes to have children (German Cancer Society, German Cancer Aid, AWMF 2018).

1.1.5.4. Targeted treatment

Unlike some cancers that exhibit oncogenic addition to one signaling cascade, endometrial carcinoma is a tumor marked by numerous gene and protein alterations that coexist and can evade targeted therapies. Finding suitable biomarkers, predictive of response to a therapeutic, will be essential in making the targeted therapies fulfill their goal.

The PI3K /AKT/mTOR signaling pathway has been reported to be frequently activated in endometrial cancer (Kanamori et al. 2001). Over the last decade this pathway has been assessed as a target for novel therapeutic strategies. *PIK3CA* mutations or loss of *PTEN* may be indicators of sensitivity to

PI3K/AKT/mTOR pathway inhibition, while activating *KRAS* mutations may predict resistance. (Janku et al. 2012; Miyake et al. 2008; Lax et al. 2000; Hayes et al. 2006). Studies have shown that endometrial tumors with *POLE* mutations and defective MMR might be excellent candidates for programmed cell death protein1 (PD-1) and programmed death-ligand 1 (PD-L1) directed immune therapies (Howitt et al. 2015). Activating *FGFR2* mutations are found in 10-16 % of primary endometrial cancers and it indicates a worse prognosis (Jeske et al. 2017). There are ongoing clinical trials on *FGFR2* inhibitor to find a better treatment for *FGFR2*-mutated or *FGFR2*-non-mutated advanced or metastatic endometrial cancer (Konecny et al. 2015).

1.2. Genomic aberrations and techniques for genetic profiling

Genomic instability is a characteristic of solid cancers, which can result in the accumulation of structural chromosome aberrations, including CNAs. There are several methods such as aCGH, Fluorescence in situ hybridization (FISH), next generation sequencing (NGS) to detect genomic aberrations. Array CGH is used as the main method in our research and is described in more detail in method section.

1.2.1. Genomic aberrations

CNVs are deletions, insertions, duplications, and more complex variations of DNA segments that is larger than 50 bp in the human genome (Girirajan et al. 2011). CNAs, which are pathogenic CNVs, accumulate somatically, emerge after many selection events and play an important role in the progressive molecular rearrangement that takes place during the cancer evolution. (Bhattacharya et al. 2020; Davoli et al. 2013). If this is the case, study methods such as aCGH may be able to detect the presence of CNAs. Identifying CNAs that are affecting important cancer genes provides useful knowledge for the development of new targeted cancer therapies or patient stratification.

In addition to CNVs, the single nucleotide polymorphism (SNP) also contributes a lot in human genomic variations. SNP is a single base locus in the genome that occurs in two allelic variants (A and B) in the population, the fact that our DNA contains one paternal and one maternal copy means that for any given SNP locus, we may obtain genotypes AA (homozygous A), AB (heterozygous), or BB (homozygous B) (van Loo et al. 2012). However, one parental copy of a region can sometimes be lost, resulting in only one copy in the region. The single copy cannot be heterozygous at SNP locations and therefore the region shows loss of heterozygosity (LOH). An LOH also exists if the remaining allele is present in multiple copies. LOH is a common molecular genetic alteration observed in cancer development. The detection of LOH could be used to identify genomic regions that contain putative tumor suppressor genes and to characterize tumor and evaluate progression (Thiagalingam et al. 2002; Zhang et al. 2012a).

1.2.2. Techniques for genetic profiling

Array CGH is a sensitive and efficient molecular cytogenetic method that serves as a detection system for the genomic alterations. It allows for a high-resolution evaluation of CNVs associated with chromosome abnormalities and it is mainly directed at detecting genomic abnormalities in cancer. Similar to conventional CGH, aCGH is based on detection of CNVs due to the ratio of fluorescent signal intensities in labeled test DNA and reference DNA. However, instead of metaphase chromosomes acting as targets for analysis, aCGH uses slides arrayed with small segments of DNA as the targets (Lucito et al. 2003).

Fluorescence in situ hybridization (FISH) is a molecular cytogenetic technique and is based on the hybridization of fluorescent probes with specific labels to a complementary DNA sequence on its corresponding sequence on the chromosome. It can detect and locate the presence or absence of specific DNA sequences on chromosomes. FISH probes have already been used for diagnosis of genetic diseases and identification of various type of cancers (Bishop 2010). Cloning vectors come in diverse seizes to suit the needs of biology and genetic research. Bacterial artificial chromosome (BAC) clones typically come in various size, generally ranging from 75 to 300 kb, while Yeast Artificial Chromosomes are ideal for very large fragments, spanning from hundreds of kilobases to megabases. Plasmids are compact, usually 1-10 kb, whereas cosmid and fosmid can carry intermediate-sized DNA fragments (35-45 kb).

NGS is a high-throughput sequencing technology which can be used to analyze DNA and RNA samples and study of genomics and molecular biology (Behjati and Tarpey 2013). Unlike aCGH method, this sequence-based approach can directly detect the nucleic acid sequence of a given DNA or cDNA molecule and makes it possible to determine related genes. Despite the costs associated with NGS have dropped a lot, arrays are still more economic and provide significant advantages when processing a large number of samples.

1.3. Aim of the study

Endometrial cancer is the most common gynecologic malignancy. Although most patients with low-grade endometrioid endometrial cancer that is amenable to treatment, patients with advanced stage or non-endometrioid types tend to have a poor prognosis. As a result, early detection by simultaneous classification of endometrial cancer is the main challenge for an adequate therapy success. Our aim was to overcome this challenge, thus, allowing further risk stratification on genetic level to guide optimal surgery, adjuvant therapy, and cancer surveillance regimes for women with endometrial cancer.

The implementation of array into clinical practice marked a new milestone for genetic diagnosis. Oligo/SNP combination array enables genome-wide detection of copy number changes and SNPs. The identification of CNAs and LOH have been integral in improving our understanding of the molecular basis for many diseases.

In order to improve the diagnosis and thus the patient's outcomes, we follow the strategy to identify cancer cells by simple techniques like FISH, obtained by brushing out of vaginal cavity. To generate suitable FISH-probes, it is necessary to know the most common imbalances in endometrial cancer. Therefore, the array has been applied for searching for aberrated regions in endometrial cancer.

The specific objectives of the thesis were:

1. Is it possible to identify endometrial cancer based on genomic imbalances?

2. Is it able to differ between type I and type II endometrial cancers by array-based CNVs?

3. Is it possible to establish a molecular classification of endometrial cancer by assessing CNVs?

2 Material and Methods

2.1. Material

2.1.1. Patient samples

65 endometrial cancer samples were collected from Kiel Biobank P2N, gynecology sub-Biobank BMB-Gyn and sub-Biobank BMB-Patho. For the use of patient material, we have received an ethics vote from the ethics committee of the Medical Faculty of the Christian-Albrechts-Universität, Kiel (D 440/17). The samples were apportioned into 30 formalin-fixed, paraffin-embedded (FFPE) tumor tissue blocks and 35 fresh tumor tissues. Sample information is listed below (Table 2.1).

Table 2.1: Information about histological type, material type and source of 65 tested endometrial cancer samples.

Case number	Histological type	Material
1	1	FFPE
2	1	fresh tissue
3	1	fresh tissue
4	1	fresh tissue
5	1	FFPE
6	1	FFPE
7	1	FFPE
8	1	FFPE
9	1	fresh tissue
10	1	fresh tissue
11	1	fresh tissue
12	1	fresh tissue
13	1	fresh tissue
14	1	fresh tissue
15	1	FFPE
16	1	FFPE
17	1	FFPE
18	1	FFPE
19	1	FFPE
20	1	FFPE
21	1	FFPE
22	1	FFPE
23	1	fresh tissue

Case number	Histological type	Material
24	1	fresh tissue
25	1	fresh tissue
26	1	fresh tissue
27	1	FFPE
28	1	FFPE
29	1	fresh tissue
30	1	fresh tissue
31	1	FFPE
32	1	fresh tissue
33	1	FFPE
34	1	fresh tissue
35	1	FFPE
36	1	FFPE
37	1	fresh tissue
38	1	fresh tissue
39	1	fresh tissue
40	1	fresh tissue
41	1	fresh tissue
42	1	FFPE
43	2	fresh tissue
44	2	fresh tissue
45	2	fresh tissue
46	2	fresh tissue
47	2	fresh tissue
48	2	fresh tissue
49	2	fresh tissue
50	2	fresh tissue
51	2	fresh tissue
52	2	FFPE
53	2	FFPE
54	2	FFPE
55	2	FFPE
56	2	FFPE

57	2	FFPE

Case number	Histological type	Material
58	2	FFPE
59	2	FFPE
60	2	FFPE
61	2	fresh tissue
62	2	fresh tissue
63	2	fresh tissue
64	2	FFPE
65	2	fresh tissue

2.1.2. Appliances

Description	Company
Tissue homogenizer, Precellys® 24	Bertin Technologies, Yvelines, France
Vortex, Vortex-Genie 2	Scientific industries Inc., Bohemia, USA
Platform shaker, Unimax 1010	Heidolph GmbH, Schwabach
Microcentrifuge, 5415R	Eppendorf, Hamburg
Thermomixer, 5436 comfort	Eppendorf, Hamburg
Fluorometer, Qubit 2.0	Life technologies corporation, Carlsbad, USA
Spectrophotometer, NanoDrop™ 2000	Thermo Fisher Scientific Inc, Waltham, USA
Focused-ultrasonicator, Covaris S220	Covaris, Woburn, USA
Vacum Centrifuge, SCANVAC SCANSPEED 40	LaboGene™, Lynge, Denmark
Carl Roth™ Micro Centrifuge	Thermo Fisher Scientific Inc, Waltham, USA
Hybridization Oven, SHEL LAB 1013	VWR International Ltd, Radnor, USA
Mini-Shaking-Hybridisierungsofen OV3	Biometra GmbH, Göttingen
SureScan Dx Microarray Scanner	Agilent Technologies, California, USA
Peltier Thermal Cycler, PTC-200	MJ Research Inc. Waltham, USA
ABI 3100 Genetic Analyzer	Applied Biosystems, Waltham, USA
Heating circulator HAAKE DC3	Gebrüder HAAKE GmbH, Karlsruhe
NoZone® Ozone Scrubber	SciGene Corporation, Sunnyvale, USA
NoZone® WS Workspace	AlphaMetrix Biotech GmbH, Rödermark
Universal 16R Centrifuge	Andreas Hettich GmbH & Co. KG, Tuttlingen
Clifton™ DuoBath™ Waterbath	Nickel Electro Ltd, Oldmixon Cres, UK

2.1.3. Materials

Description	Company
GenetiSure Unrestricted aCGH +SNP (4x180 k)	Agilent Technologies, California, USA
Micro tubes (0.5ml, 1,5ml)	Sarstedt, Nümbrecht
PCR SingleCap 8er-Softstrips 0.2mL	Biozym Scientific GmbH, Oldendorf
Hybridization Gasket Slide Kit	Agilent Technologies, California, USA
Hybridization Chamber	Agilent Technologies, California, USA
SureScan Slide Holders	Agilent Technologies, California, USA
Multiply PCR plate(96-well)	Sarstedt, Nümbrecht
Pipettor, Research	Eppendorf, Hamburg

Pipette Tips	Sarstedt, Nümbrecht

2.1.4. Chemicals, reagents, substrates, kits

Chemicals, reagents, substrates	Company
Dulbecco's-Phosphate Buffered Saline (PBS)	Gibco®, Life Technologies, Darmstadt
Ethanol pure	Carl Roth GmbH, Karlsruhe
Reference Female DNA, 5190-8850	Agilent Technologies, California, USA
Human Cot-1 DNA™, 15279011	Thermo Fisher Scientific Inc, Waltham, USA
Agilent Oligo aCGH/ChIP-on-Chip Wash Buffer 1	Agilent Technologies, California, USA
Agilent Oligo aCGH/ChIP-on-Chip Wash Buffer 2	Agilent Technologies, California, USA
AmpliTaq Gold® DNA Polymerase (5 U/µl)	Thermo Fisher Scientific Inc, Waltham, USA
Hi-Di™ formamide	Thermo Fisher Scientific Inc, Waltham, USA
LiChrosolv® Water for chromatography	Merck KGaA, Darmstadt

Kits	Content	Company
QIAamp® DNA Mini Kit (Cat No.51304)	QIAamp Mini Spin Columns	Qiagen, Hilden
	Collection Tubes (2 ml)	
	Buffer AL	
	Buffer ATL	
	Buffer AW1 (concentrate)	
	Buffer AW2 (concentrate)	
	Buffer AE (10 mM Tris-Cl, 0.5 mM EDTA; pH 9.0)	
	Proteinase K	
BIOstic® FFPE Tissue DNA Isolation Kit (Cat No.12250-50)	Solution FP1	MO BIO Laboratories, Inc, Qiagen, Hilden
	Solution FP2	
	Solution FP3 (Proteinase K)	
	Solution FP4 (chaotropic salt buffer)	
	Solution FP5 (100 % ethanol)	
	Solution FP6 (wash buffer)	
	Solution FP7 (ethanol-based wash buffer)	
	Solution FP8 (10 mM Tris pH 8.0)	
	Spin Filters	
	2 ml Collection Tubes	
QIAGEN® GeneRead DNA FFPE Kit (Cat No.180134)	QIAamp MinElute® Columns	Qiagen, Hilden
	Collection Tubes	
	Deparaffinization Solution	
	Buffer FTB	
	Buffer AL	
	Proteinase K	
	Buffer AW1 (concentrate)	

	Buffer AW2 (concentrate)	
	Uracil-N-glycosylase	
	RNase-Free Water	
	RNase A (100 mg/ml)	
	Buffer ATE (10 mM Tris-Cl pH 8.3, 0.1 mM EDTA, 0.04 % NaN3)	
Qubit dsDNA BR Assay Kit (Cat. No. Q32850)	Qubit® dsDNA BR Reagent (Component A)	Thermo Fisher Scientific Inc, Waltham, USA
	Qubit® dsDNA BR Buffer (Component B)	
	Qubit® dsDNA BR Standard #1 (Component C)	
	Qubit® dsDNA BR Standard #2 (Component D)	
CytoSure Genomic DNA Labelling Kit (Cat. No. 020020)	Reaction Buffer	Oxford Gene Technology, Oxfordshire, UK
	Random Primer	
	Cy3-dCTP	
	Cy5-dCTP	
	dCTP Labelling Mix	
	Control DNA	
	Klenow	
	Nuclease-Free Water	
	purification columns	
	collection tubes	
Oligo aCGH/ChIP-on-Chip Hybridization Kit	2X Hi-RPM Hybridization Buffer	Agilent Technologies, California, USA
	10X Oligo aCGH/ChIP-on-Chip Blocking Agent	
MSI Analysis System, version 1.2	MSI 10X Primer Pair Mix	Promega, Madison, USA
	Gold ST*R 10X Buffer	
	Nuclease-Free Water	
	K562 High Molecular Weight DNA (10ng/µl)	
	Internal Lane Standard 600	

2.1.5. Software

Description	Company
Agilent Feature Extraction Software 3.0.5.1	Agilent Technologies, California, USA
CytoSure Interpret Software 4.8.32	Oxford Gene Technology, Oxfordshire, UK
GeneMapper 4.0	Applied Biosystems, Waltham, USA
Date collection software v3.0	Applied Biosystems, Waltham, USA

2.2. Methods

2.2.1. Array design

Genomic data from the TCGA support classification of endometrial cancer into four prognostically significant subgroups, each subgroup has specific characteristics and signature genes. We targeted 13 relevant genes, which are distributed differently in the four groups and may help us to classify endometrial cancer at the molecular level (Table 1.3). With the support of Oxford Gene Technology (OGT), we devised aCGH +SNP array (1500-KIE; design_0001 Additional *POLE*; CGH+SNP 4x180k Array) that analysis of CNV and LOH combined in a single assay. In order to cover imbalances of genes suspicious in endometrial cancer, the design was fitted with increased resolution for these 13 genes (Table 2.2).

Table 2.2: Gene list of customized high-resolution-array.

Gene	Chromosome	Start position	Stop position
AR1D1A	chr1	27022402	27108721
CTNNB1	chr3	41236208	41301707
PIK3CA	chr3	178865782	178958001
FBXW7	chr4	153242290	153457373
APC	chr5	112043075	112182056
PTEN	chr10	89622750	89731807
FGFR2	chr10	123237724	123358092
KRAS	chr12	25357603	25403990
POLE	chr12	133200224	133264170
BRCA2	chr13	32889491	32973929
ZFHX3	chr16	72816664	73093717
TP53	chr17	7564977	7590988
SPOP	chr17	47676126	47755716

2.2.2. DNA extraction

2.2.2.1. gDNA extracted from fresh tissue

QIAamp® DNA mini kit was used to extract gDNA from fresh tissue. The fresh tissue (up to 25 mg) was removed from storage and placed in a 1.5 ml microcentrifuge tube which contains no more than 80 µl PBS. The sample was homogenized using the tissue homogenizer. 100 µl buffer ATL and 20 µl proteinase K were added, mixed under vortex and then incubated at 56 °C on a platform shaker until the tissue was completely lysed (normally 1-3 hours). 200 µl buffer AL was added to the sample, mixed by pulse-vortexing for 15 seconds and incubated at 70 °C for 10 minutes. 200 µl ethanol (96-100 %)

was added to the sample and mixed by pulse-vortexing for 15 seconds. The lysate was transferred to the QIAamp mini spin column (in a 2 ml collection tube) and centrifuged at 6000 × *g* for 1 minute. The QIAamp mini spin column was placed in a newly provided collection tube. 500 µl buffer AW1 was added into the QIAamp mini spin column, spun at 6000 × *g* for 1 minute. The QIAamp mini spin column was placed in a 2 ml newly provided collection tube. 500 µl buffer AW2 was added into the QIAamp mini spin column, centrifuged at full speed (13,000 × *g*) for 3 minutes. QIAamp mini spin column was again transferred in a new 1 ml collection tube and centrifuged at full speed for 1 minute. QIAamp mini spin column was then placed in a 1.5 ml microcentrifuge tube, 200 µl buffer AE was added into the spin column.

2.2.2.2. gDNA extracted from FFPE tissue

Based on the protocol BIOstic® FFPE tissue DNA isolation kit, the procedure is as follows:

180 µl of solution FP1 and 20 µl of solution FP2 were added together to a 1.5 ml microcentrifuge tube which contains 1 or more FFPE tissue slices (up to 15 mg). 20 µl solution FP3 was added into the tube and mixed well under vortex. Samples were incubated at 55 °C for 1 hour, then transferred to the heat block set to 90 °C and incubated for 1 hour. Samples were centrifuged at 13,000 × *g* for 1 minute and the digested lysate was transferred to a newly provided 2 ml collection tube. 200 µl of solution FP4 and 200 µl of solution FP5 were sequentially added to the 2 ml collection tube and thoroughly mixed under vortex. The entire lysate (620 µl) was loaded onto the spin filter and centrifuged at 10,000 × *g* for 1 minute. The filtrate was discarded, and the column was back into the collection tube. The spin filter was washed with 500 µl of solution FP7 and centrifuged at 10,000 × *g* for 1 minute, the filtrate was discarded. The spin filter was spun for 2 minutes at full speed and transferred to a new 2 ml provided collection tube. 50-100 µl of Solution FP8 was directly added to the column membrane. The column was then incubated at room temperature for minimum 5 minutes and centrifuged at 10,000 × *g* for 1 minute. Elute was then transferred to a new clean microcentrifuge tube and quantified.

Based on the protocol QIAGEN ® GeneRead DNA FFPE kit, the procedure is as follows:

FFPE tissue was cut with a thickness up to 10 µm and put it into a 1.5 ml microcentrifuge tube. 160 µl deparaffinization solution was added into the tube and mixed for 10 seconds under vortex. The sample was then incubated at 56 °C for 3 minutes and cooled at room temperature. 55 µl RNase-free water, 25 µl buffer FTB, and 20 µl proteinase K were added sequentially to the tube, mixed well under vortex, incubated at 56 °C for 1 hour, then transferred to the heat block set to 90 °C and incubated for 1 hour. The lower, clear phase was transferred into a new microcentrifuge tube. 115 µl RNase-free water and 35 µl Uracil-N-glycosylase were added to the sample sequentially and mixed under vortex, incubated at 50 °C for 1 hour. 2 µl RNase A was added to the sample and mixed, incubated for 2 minutes at room temperature. 250 µl buffer AL and 250 µl ethanol (96-100 %) were added to the sample sequentially

and mixed by vortex. 700 µl lysate was transferred to the QIAamp MinElute® column and spun at maximum speed for 1 minute, the filtrate was discarded and collection tube was reused. This step was repeated until the complete lysate was used. 500 µl buffer AW1 was then added to the spin column and centrifuged at maximum speed for 1 minute, the filtrate was discarded and collection tube was reused. 500 µl buffer AW2 and 250 µl ethanol (96-100 %) were added separately to the spin column and handled in the same way as 500 µl buffer AW1. The spin column was transferred to a new provided 2 ml collection tube and centrifuged at maximum speed for 1 minute. The QIAamp MinElute® column was placed in a newly 1.5 microcentrifuge tube. 20-40 µl buffer ATE was directly added to the column membrane. The sample was incubated at room temperature for 1 minute and centrifuged at maximum speed for 1 minute. Elute was then transferred to a new clean centrifuge tube and quantified.

2.2.3. Quantification and qualification of DNA

Qubit dsDNA BR assay kit was used to quantify the DNA. Qubit® working solution was prepared by diluting the Qubit® dsDNA BR reagent 1:200 in Qubit® dsDNA BR buffer. 190 µL of Qubit® working solution and 10 µL of each Qubit® standard were sequentially added to a 0.5 ml micro tube. 199 µL Qubit® working solution and 1 µl sample DNA to individual assay tubes so that the final volume was 200 µL, then mixed by vortexing 2–3 seconds. All tubes were incubated at room temperature for 2 minutes. The “Standards” screen was displayed on the home screen of the Qubit® 2.0 fluorometer by choosing “dsDNA Broad Range” as the assay type. Calibration was then completed by reading tubes containing standard #1 and standard #2, respectively. “Read sample” screen was then displayed, each sample was read two times and the quantification of the samples was calculated based on the better read of every two readings of each sample. To calculate the concentration of sample, the following equation was used:

$$Concentration\ of\ sample\ = \frac{200 \times QF\ value}{x}$$

where QF value is the value given by the Qubit® 2.0 fluorometer and x is the number of microliters of sample added to the assay (µg/mL).

The quality of extracted DNA was also measured by using spectrophotometer NanoDrop™ 2000. The spectrometer was blanked with 1.5 µl of water. Then 1.5 µl of sample DNA was subsequently placed on top of the detection surface and scanned. The 260/280 and 230/260 wave lengths were recorded for each sample. The acceptable 260/280 ratio exceeds 1.8 and ideally the 260/230 ratio should also exceed 1.5.

2.2.4. DNA labeling

Equivalent amounts of patient and reference DNA (500-1000 ng) were labelled by random primer with either Cy3-dCTP or Cy5-dCTP using the CytoSure Genomic DNA labelling kit. Patient samples were labelled with Cy3-dCTP and reference DNAs were labeled with Cy5-dCTP. Normal Agilent female DNA was used as reference DNA for fresh patient samples. According to the protocol in Table 2.3, reference DNA of FFPE samples were prepared by shearing Agilent female DNA with focused-ultrasonicator Covaris S220, the target peak for base pair size is 150 bp to 200 bp.

Table 2.3: Agilent female DNA shearing protocol.

Parameter	**Settings**
Sample Type	Agilent Female DNA
Duty Cycle	10 %
Peak Power	175
Cycles per Burst	200
Timer	6 cycles of 1 minute each
Temperature	5 to 25 ℃

The amount of DNA required for the equivalent of 500-1000 ng were calculated for each sample and the appropriate amount was transferred into a 0.2 ml PCR tube, nuclease-free water was added until get a volume of 18 µl. 10 µl random primer and 10 µl reaction buffers were added to each tube and mixed by flicking the tube, then centrifuged for 15 seconds. The tubes were denatured in a PCR block with heated lid for 20 minutes at 99 °C for fresh tissue samples and reference DNAs, 3 minutes at 95 °C for FFPE samples and shredded reference DNAs, then immediately placed on ice for 5 minutes.

12 µl of dCTP labeling mix/ Cy3/5-dCTP/Klenow master mix (on ice) was added to each tube using the volumes illustrated in Table 2.4 as a guidance. Tubes were mixed by flicking and shortly spun (< 10 seconds). All tubes were incubated at 37 °C for 2 hours, 65 °C for 10 minutes, then placed on ice for 5 minutes followed by 15 seconds of centrifugation.

Table 2.4: dCTP labeling mix/ Cy3/5-dCTP/Klenow master mix.

	Sample	**Reference**
dCTP labelling mix	10 µl	10 µl
Cy3-dCTP	1 µl	-
Cy5-dCTP	-	1 µl
Klenow	1 µl	1 µl

2.2.5. Purifying the labeled target

Two purification columns (supplied in the CytoSure Genomic DNA Labelling Kit) were prepared by vortexing the resin briefly. The cap was loosened one-quarter turn and the bottom closure was snapped off. The column was placed in a collection tube and pre-spun the column for 1 minute at 2,000 x *g*. The spin column was removed from the tube and placed in a fresh microcentrifuge tube, the eluate was discarded. Samples were added to the center of the resin and centrifuged at 2,000 x *g* for 1 minute, the final volume should be ~45 µl. The concentration of each sample was measured using the NanoDrop™ 2000. DNA concentrations greater than 225 ng/µl and dye concentrations greater than 2.6 pmol/µl were considered adequate to continue with array. The labeled targets were combined together and dried to ~39 µl by SpeedVac vacuum concentrator.

2.2.6. Hybridization of arrays with labelled target

The 10x blocking agent was prepared by adding 1,350 µl water to the 10x Blocking Agent tube (supplied) and incubated at room temperature (15-25 °C) for 60 minutes. The hybridization master mix was prepared as suggested in Table 2.5. Seventy-one µl of the master mix was added to each sample and mixed thoroughly by pipetting. The target was denatured at 94 °C for 3 minutes and incubated at 37 °C for 30 minutes, then spun down for 10 seconds.

Table 2.5: Hybridization Master Mix.

	Volumes required for each 110 µl hybridization mix	**Volumes for master mix (4x) ***
Cy3 and Cy5-labelled genomic DNA	39 µl	–
Cot-1 (1 mg/ml)	5 µl	25 µl
Agilent 10x Blocking Agent	11 µl	55 µl
Agilent 2x HiRPM Hybridization Buffer	55 µl	275 µl

The Agilent hybridization gasket was placed into an Agilent chamber base, 100 µl of the hybridization mix was pipetted onto each chamber of the gasket slide. The CGH+SNP array was placed onto the gasket slide. The clamp was placed on the slide and thumbscrew tightened firmly, then the hybridization chamber placed in the hybridization oven at 65 °C for 22 hours at a speed of 20 rpm.

2.2.7. Washing and scanning of arrays

Wash buffer 2 and containers were pre-warmed overnight at 37 °C. The slide was placed in the disassembly bath (filled with wash buffer 1) and the gasket slide was prized from the Cytosure array under the surface of the buffer. The slide was then transferred quickly to the wash buffer 1 bath, which was placed a stirring flea, stirred at room temperature for 5 minutes. The slide was then changed

quickly into the pre-warmed wash buffer 2 bath and stirred at 37 °C for exactly 1 minute. The slide was then dried under ozone-free air and placed into the Agilent slide holder and scanned by SureScan Dx Microarray Scanner. Figure 3 is a sample of array scanned image.

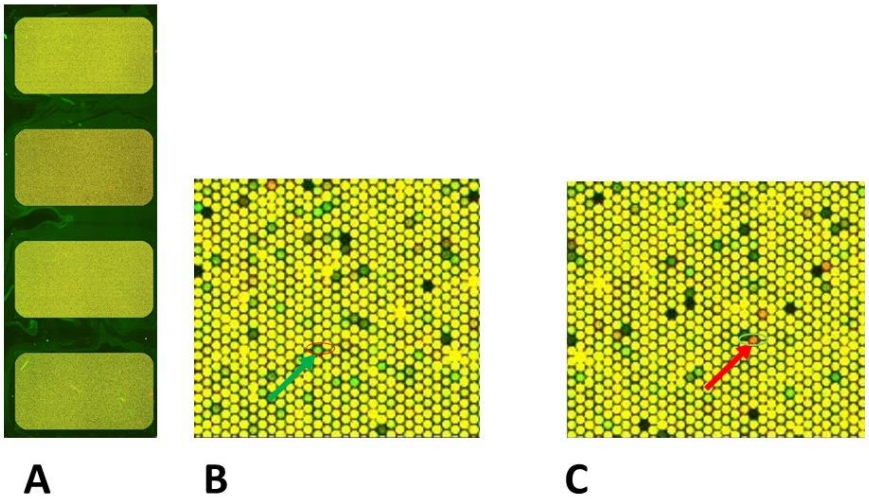

Figure 3: SureScan Dx Microarray Scanner Raw Image. Equal hybridization of both tumor and reference DNA are indicated by yellow spots while control spots with no hybridization of DNA are indicated by blank spots.
A. CGH+SNP array 4x180K scan; B. Increased hybridization of patient DNA representative of a gain indicated by green spot and green arrow; C. Decreased hybridization of patient DNA representative of a deletion indicated by a red spot and red arrow.

2.2.8. Data generation and computer analysis

The scanned image was extracted using Agilent Feature Extraction Software 3.0.5.1. Quality of the hybridization was assessed using the Feature Extraction Quality Control (QC) report, which sets the derivative log 2 ratio spread below 0.2. QC reports were used to confirm array processing results, verify reliability of image processing results, detect common array hybridization or washing artifacts. The QC-metrics table was also used to check signal intensities and background noise. Figure 4 shows a screen shot of the QC report. Data analysis has been performed using the CytoSure Interpret Software. Annotations are based on the Human and the results were displayed. Gene contents of aberrations were cross-checked with the UCSC (http://www.genome.ucsc.edu) and Ensemble databases (http://www.ensembl.org). Figure 5 displays a representative array plot and Figure 6 shows a table views of a tested sample, both figures are generated by CytoSure Interpret Software 4.8.32.

QC Report - Agilent Technologies : 2 Color CGH

Date	Thursday, October 20, 2016 - 11:54	Sample(red/green)	
User Name	Admin	FE Version	12.0.3.1
Image	SG15435056_257581310100_S001 [1_3]	BG Method	Detrend on (NegC)
Protocol	CGH_1200_Jun14 (Read Only)	Multiplicative Detrend	True
Grid	CytoSure 4x180k+LOH	Dye Norm	Linear
Saturation Value	65526 (r), 65526 (g)		
DyeNorm List	NA		
No of Probes in DyeNorm List	NA		

Spot Finding of the Four Corners of the Array

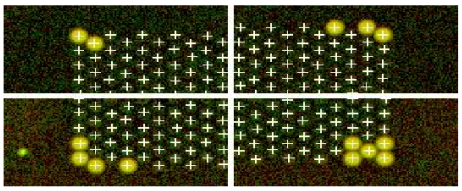

Grid Normal

Outlier Numbers with Spatial Distribution

1064 rows x 170 columns

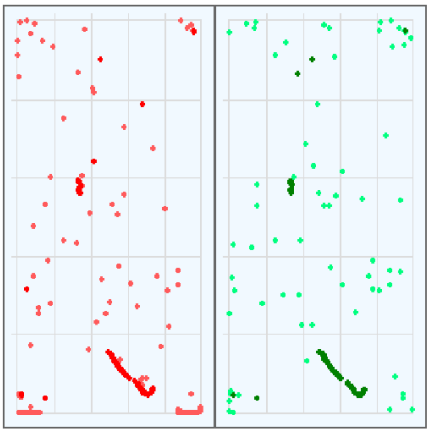

Red FeaturePopulation Red Feature NonUniform
Green FeaturePopulation Green Feature NonUniform

Feature	Red	Green	Any	%Outlier
Non Uniform	112	108	137	0.08
Population	146	74	197	0.11

Evaluation Metrics for CGH_QCMT_Jun14
Excellent (7) ; Good (5) ; Evaluate (1)

Metric Name	Value	Excellent	Good	Evaluate
IsGoodGrid	1.00	>1	NA	<1
AnyColorPrcntFeatNonU...	0.08	<1	1 to 5	>5
DerivativeLR_Spread	0.23	<0.20	0.20 to 0.30	>0.30
gRepro	0.05	0 to 0.05	0.05 to 0.20	<0 or >0.20
g_BGNoise	5.91	<5	5 to 15	>15
g_Signal2Noise	163.82	>100	30 to 100	<30
g_SignalIntensity	968.91	>150	50 to 150	<50
rRepro	0.06	0 to 0.05	0.05 to 0.20	<0 or >0.20
r_BGNoise	5.51	<5	5 to 15	>15
r_Signal2Noise	173.26	>100	30 to 100	<30
r_SignalIntensity	954.61	>150	50 to 150	<50
RestrictionControl	-1.00		0.80 to 1	<0.80 or >1
LogRatioImbalance	-0.02	-0.26 to 0.26	(-0.75 to -0.2...	<-0.75 or >0.75

• Excellent • Good • Evaluate

Histogram of Signals Plot (Red)

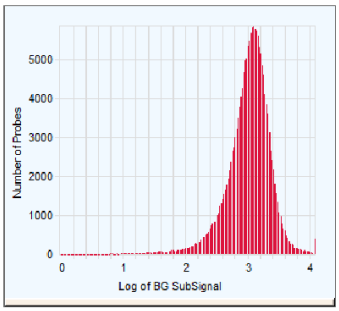

Histogram of Signals Plot (Green)

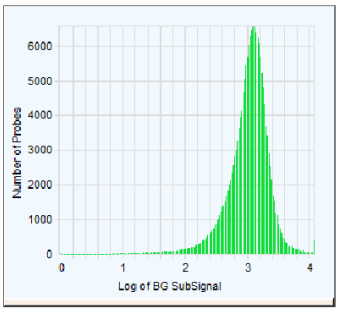

Spatial Distribution of the Positive and Negative LogRatios

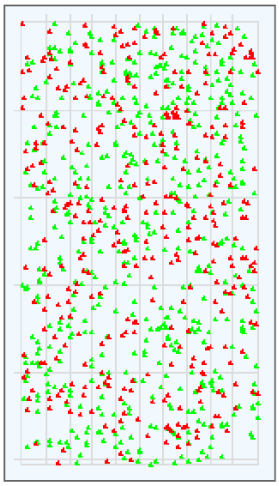

#Positive:7861 (Red) ; #Negative:9760 (Green)

•Positive •Negative

Positive: 4.58% of NonCtrl Features : Random (Value 0.98)
Negative: 5.69% of NonCtrl Features : Random (Value 0.98)

Red and Green Background Corrected Signals (Non-Control Inliers)

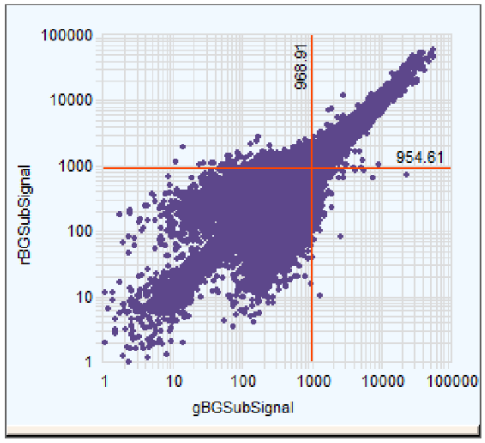

Features (NonCtrl) with BGSubSignals < 0: 29 (Red); 46 (Green)

Figure 4: Screen shot of the Feature Extraction Quality Control report.

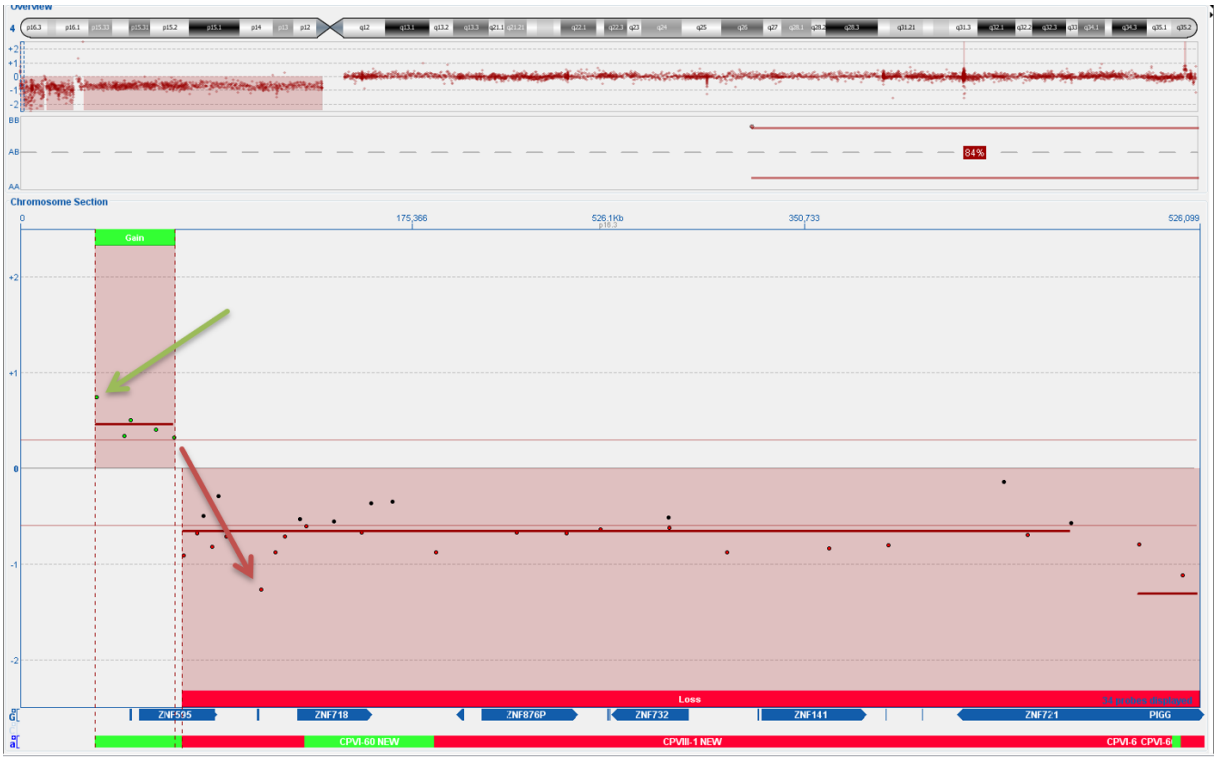

Figure 5. CytoSure Interpret Software Output, array plot illustrates identical gains and losses. Green arrow pointed a gain and red arrow represented a loss.

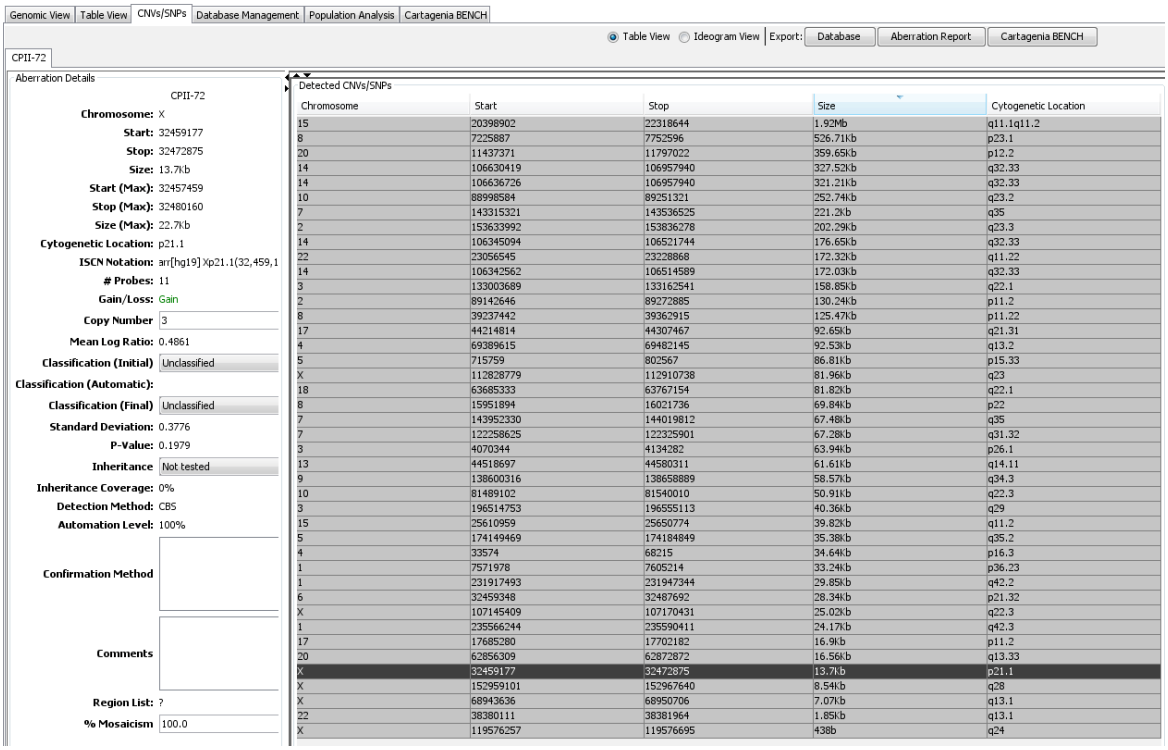

Figure 6: CytoSure Interpret Software Output, table view of a tested sample. Information regarding copy number variants, known pathogenicity, size, and location are provided.

2.2.9. Assessing of MSI using the panel of 5 mononucleotide repeats loci

The detection of MSI was conducted with MSI Analysis System, which includes 5 mononucleotides repeat markers (BAT-25, BAT-26, NR-21, NR-24 and MONO-27) and 2 pentanucleotide repeat markers (Penta C and Penta D). Amplification Mix for the MSI Analysis System for the volume of 2 µl in a 10 µl reaction volume was prepared using the protocols detailed below (Table 2.6):

Table 2.6: Amplification Mix for the MSI Analysis System

Component	Volume Per Reaction
Nuclease-Free Water	5.85 µl
Gold ST* R 10X Buffer	1.00 µl
MSI 10X Primer Pair Mix	1.00 µl
AmpliTaq Gold® DNA Polymerase (5 U/µl)	0.15 µl
Total reaction volume	8.00 µl

8 µl of amplification mix was transferred to the PCR tube, 2 µl of gDNA (2 ng) for was added to the tube containing amplification mix, mixed by pipetting several times. For the positive amplification control, the K562 high molecular weight DNA was diluted 1:10 to 1 ng/µl in nuclease-free water and 2 ng diluted DNA added to the amplification mix, for the negative amplification control, 2 ng nuclease-free water was added to the amplification mix.

The 96-well reaction plate was placed in the PCR thermal cycler and the bellowed cycling profile was implemented as shown in Figure 7:

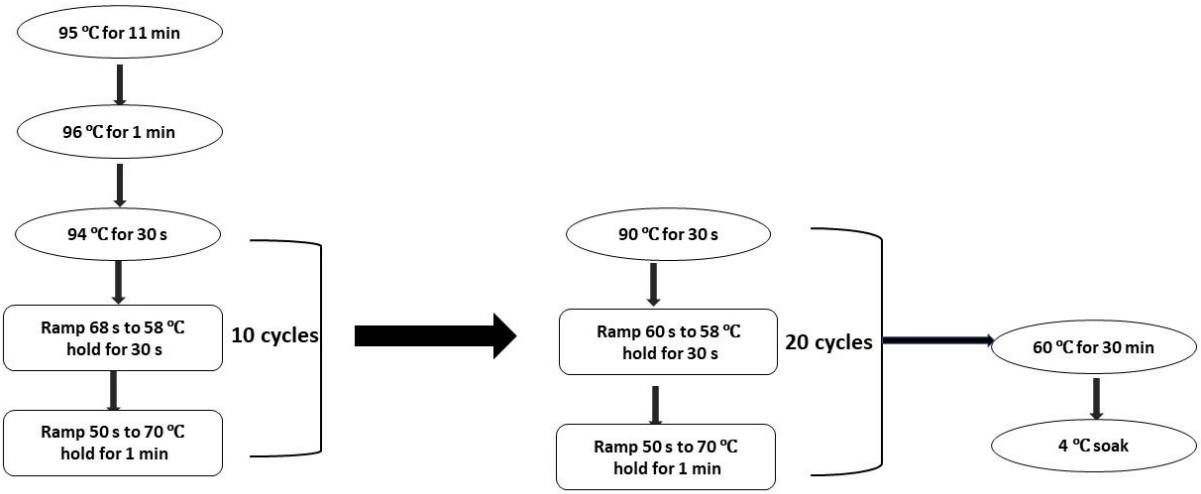

Figure 7: Details of thermal profile for DNA amplification using PCR.

A loading cocktail was prepared as follows and vortexed for 10-15 seconds:

[(0.5 µl ILS 600) + (9.5 µl Hi-DiTM formamide)] x (#injections)

10 µl of formamide/internal lane standard mix was pipetted into each well and 1 µl of amplified sample was then added. The wells were covered with septa and briefly centrifuged, then denatured at 95 °C for 3 minutes and immediately chilled on ice for 3 minutes. The samples were then analyzed by an ABI 3100 Genetic Analyzer equipment. The evaluation of the data was done with the GeneMapper 4.0 software. Detection of MSI is based on comparing allelic profiles generated by amplifying matching normal and tumor sample DNA. The appearance of novel alleles in the tumor sample indicates microsatellite instability. MSI is defined when ≥ 40 % markers show instability in tumor DNA, samples with less than 40 % mononucleotide repeat markers altered be classified as MSS (Figure 8).

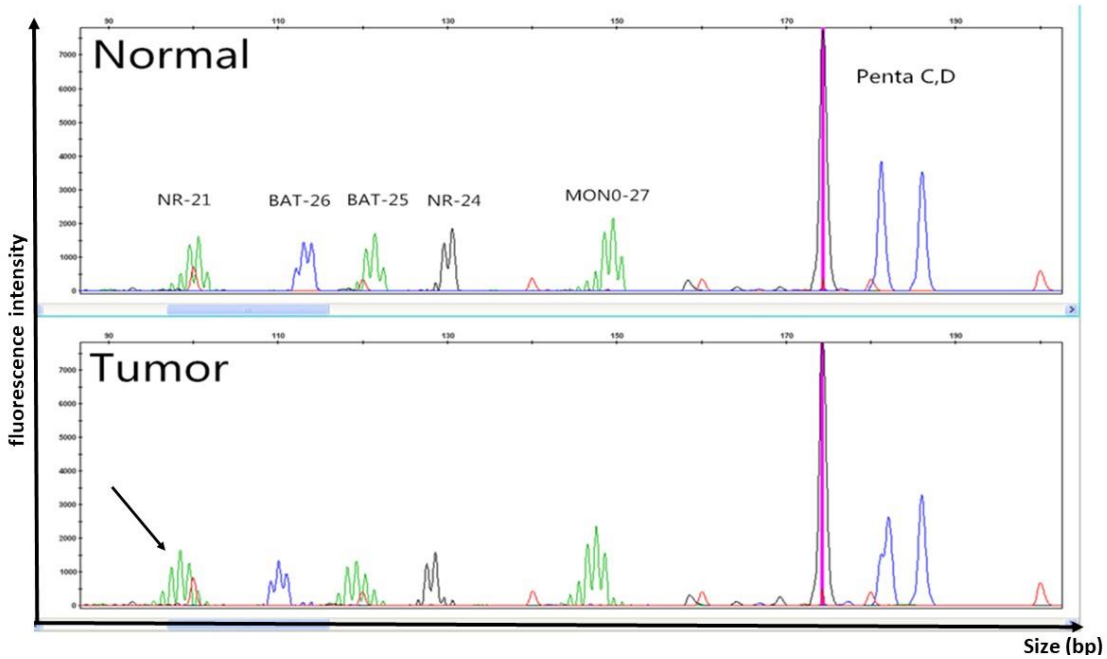

Figure 8: Capillary electrophoresis results of the MSI Analysis System.
Red peaks are internal size standards. Green, blue, and black peaks are amplification products from microsatellite loci. An example of one shifted locus is demonstrated (arrow) in the tumor sample.

2.3. Statistical analyses

Differences in frequencies of parameters were calculated using the chi-square test with or without Fisher's exact test. Differences were regarded as statistically significant for $p<0.05$. Descriptive values were presented as median and range. Excel statistical software was used to analyze the data.

3 Results

3.1. Copy number variation

CNV is a large part of structure variation, whereby whole or parts of chromosomes are deleted or amplified. It has higher mutation rates than SNP and affects large fragments of genome. Thus, CNV correlates with the development of cancer and can therefore be used as a strategy to identify novel markers or mechanisms that are susceptible to cancer. In this study 65 endometrial cancer samples were examined using aCGH. Figure 9 displays the total number of regions in which the chromosomal copy number was abnormal. The overall screen shot detects that aberrations were found in different cases in the same places. However, it is apparent that the specific aberrant locations and the number of aberrations were difficult to be obtained in this picture. Figure 10 shows the frequency of copy number gains in all recruited tumor samples. Closer examination of the data, the minimal overlapping regions of most frequent gains are showed in Table 3.1. The regions at 3p22.1, 5q22.2, 4q31.3, 10q26.13 were gained in more than 50 % of our endometrial cancer patients, 1q21.1, 3q26.32, 4p16.3, 5q15, 7q35, 10q23.31, 12p12.1, 13q13.1, 15q11.2, 15q26.1, 16q22.2 and 17q21.33 gained in 32.3 % - 44.6 % of 65 patients.

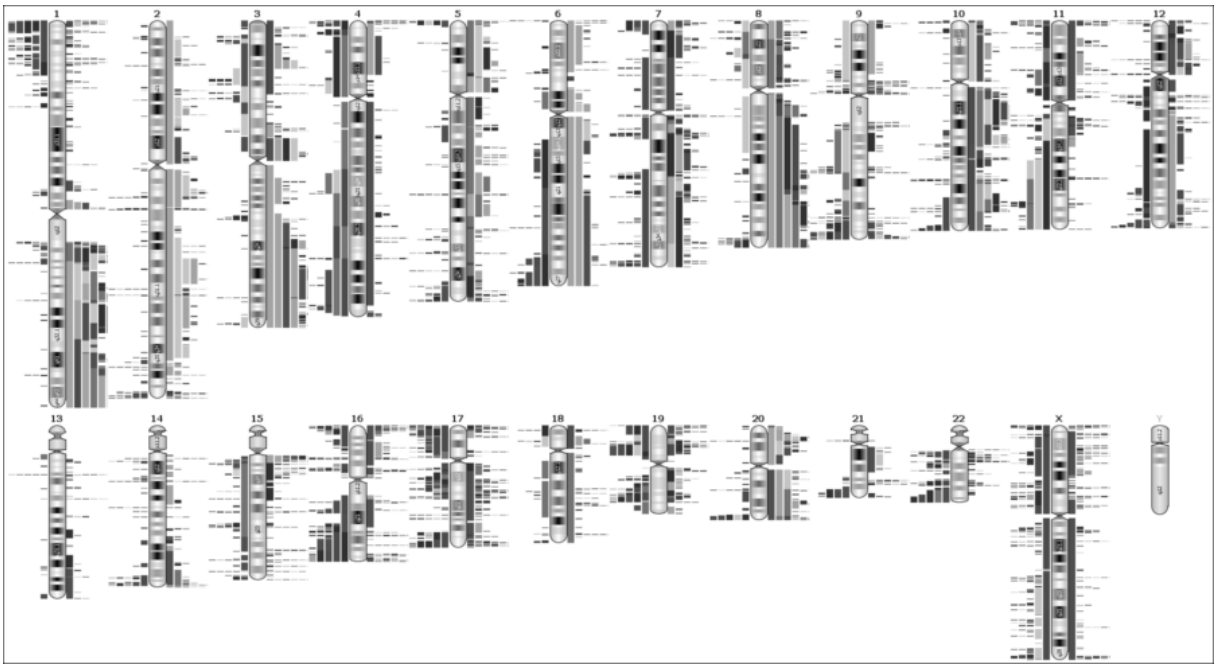

Figure 9. Overview of copy number aberrations in endometrial cancer were generated using CytoSure interpret software. The Ideogram represents the global CNVs which were manifested across the whole genome of the recruited 65 tumor samples. Each columnized line denotes a single sample, in which all chromosomes were shown to display CNVs. Positions showing losses are on the left side of the chromosome whereas gains are on the right side.

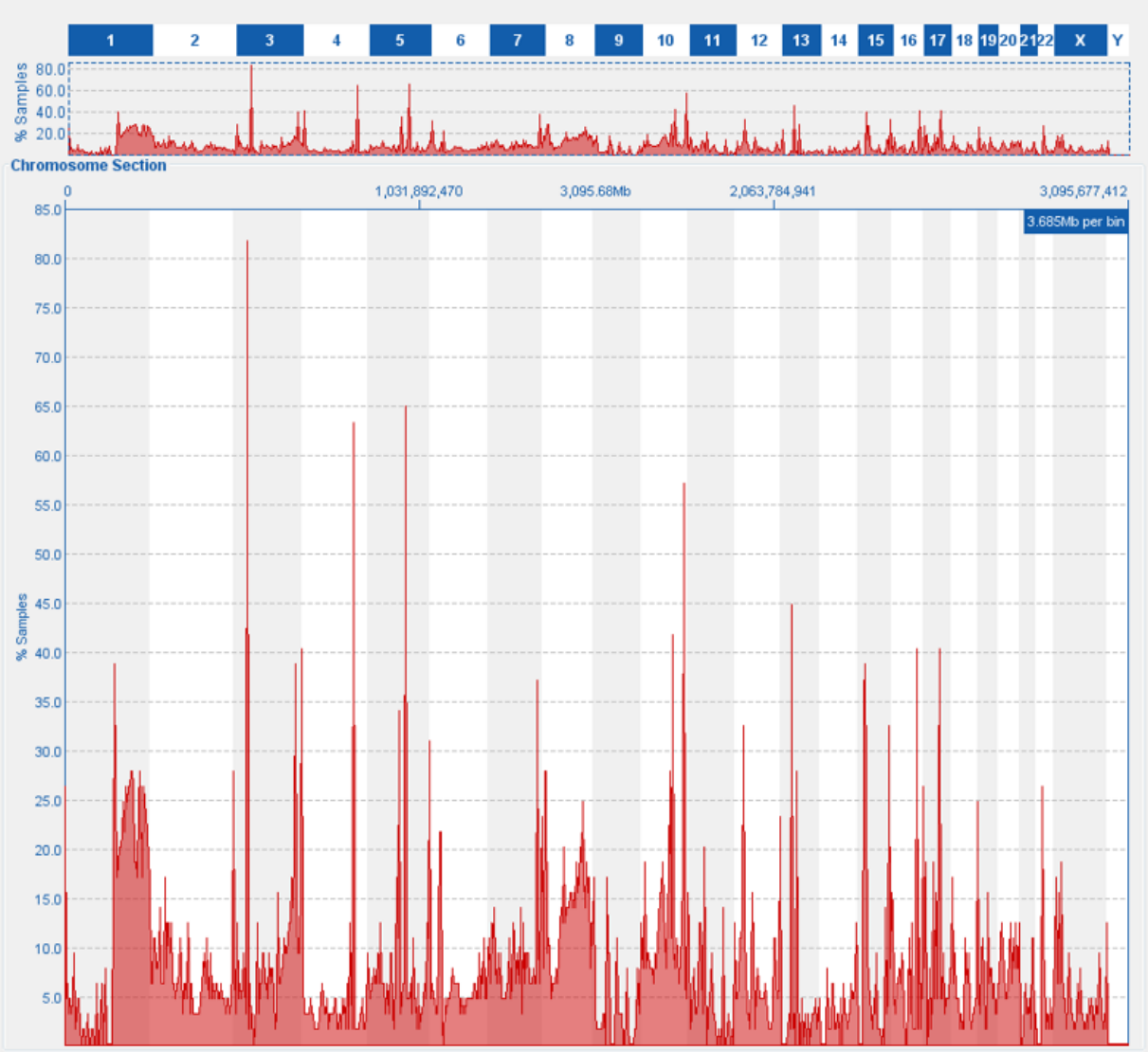

Figure 10. Frequency of copy number gains in 65 endometrial cancer samples.

Table 3.1. The minimal overlapping regions of most common copy number gains detected by aCGH in 65 patients with endometrial cancer.

Chromosomal location	Start (bp)	Stop (bp)	Size (Kb)	Patients with gains		Representative genes*
				Number	Percentage [%]	
3p22.1	41281477	41281777	0.3	53	81.5	*CTNNB1*
4q31.3	153269677	153269977	0.3	42	64.6	*FBXW7*
5q22.2	112164360	112164659	0.3	42	64.6	*APC*
10q26.13	123237773	123238072	0.3	37	56.9	*FGFR2*
4q31.3	153332101	153332434	0.3	36	55.4	*FBXW7*
10q26.13	123238662	123238961	0.2	34	52.3	*FGFR2*

Chromosomal location	Start (bp)	Stop (bp)	Size (Kb)	Patients with gains		Representative genes*
				Number	Percentage [%]	
13q13.1	32900128	32900427	0.3	29	44.6	*BRCA2*
10q23.31	89685180	89685480	0.3	27	41.5	*PTEN*
13q13.1	32950650	32950950	0.3	27	41.5	*BRCA2*
17q21.33	47713706	47714268	0.6	27	41.5	*SPOP*
4p16.3	44394	59942	15.2	26	40.0	
16q22.2	72818203	72821070	2.8	26	40.0	*ZFHX3*
1q21.1	145805123	145883187	76.2	25	38.5	
3q26.32	178928017	178928317	0.3	25	38.5	*PIK3CA*
3q26.32	178937437	178937736	0.3	24	38.5	*PIK3CA*
7q35	143315179	143536260	215.9	25	38.5	
15q11.2	22683827	22717524	32.9	25	38.5	
15q11.2	23432887	23596399	159.7	25	38.5	
17q21.33	47676904	47677364	0.5	25	38.5	*SPOP*
16q22.3	73092864	73093164	0.3	24	37.0	*ZFHX3*
10q26.13	123285513	123285812	0.3	23	35.4	*FGFR2*
15q11.2	20759256	22319603	1523.8	23	35.4	
5q15	92922322	92922819	0.5	22	33.4	*NR2F1*
13q13.1	32918537	32918836	0.3	22	33.8	*BRCA2*
12p12.1	25362434	25362734	0.3	21	32.3	*KRAS*
13q13.1	32906474	32906774	0.3	21	32.3	*BRCA2*
15q26.1	93428882	93435270	6.2	21	32.3	

*Representative genes are the endometrial cancer related genes encompassed in the region.

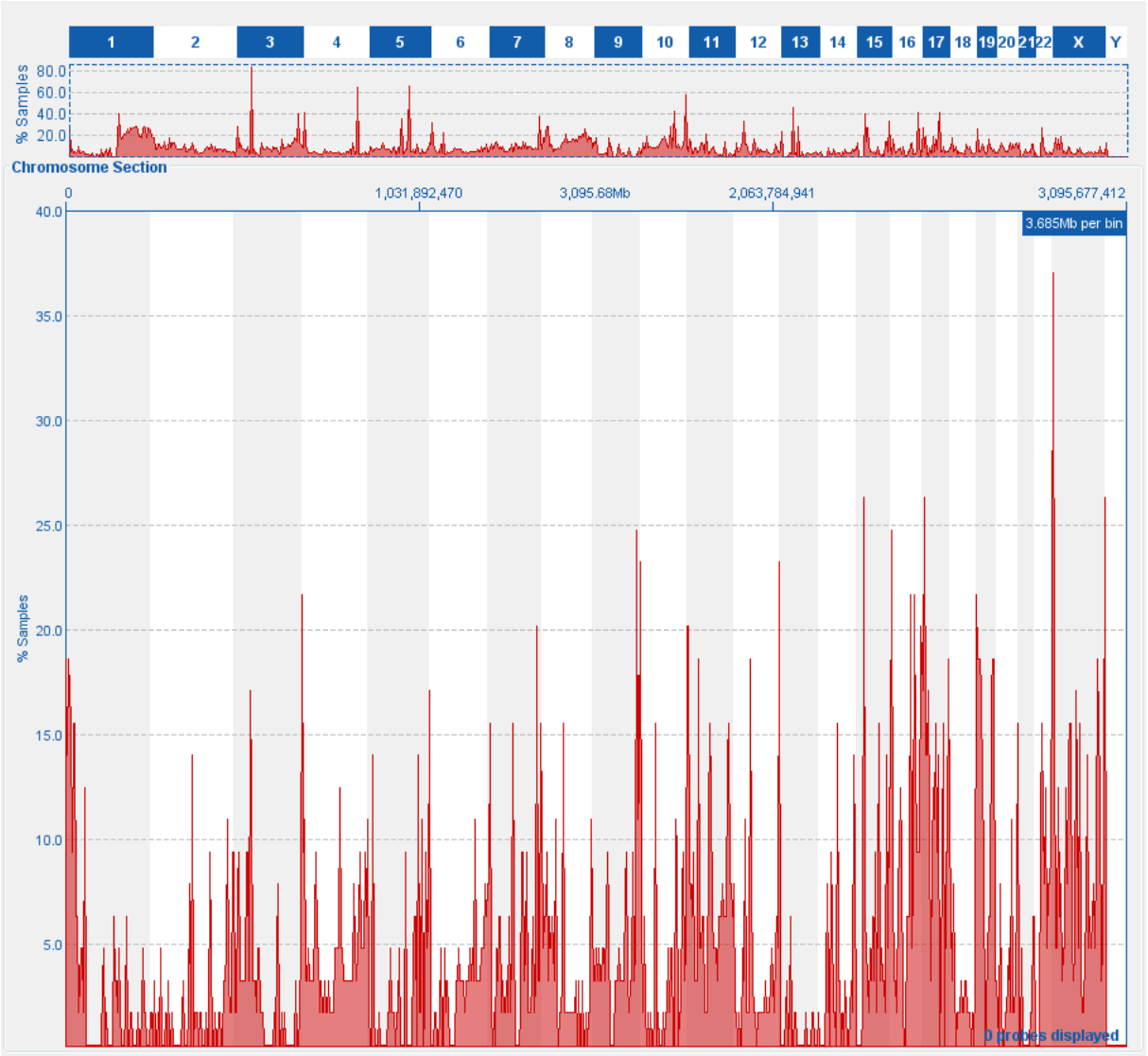

Figure 11. Frequency of copy number losses in 65 endometrial cancer samples.

Figure 11 displays the overview of the frequency of copy number losses in all endometrial cancer samples. To gain further insight, we listed the minimal overlapping regions of most frequent losses in Table 3.2. The regions at Xq22.33 were lost in 36.9 % and the regions 4p16.3, 9q34.3, 12q24.33, 15q11.2, 16p13.3, 16q12.2, 16q22.1, 16q24.2q24.3, 17p13.1, 19p13.2, 19p13.3, Xq28 in 20 %-26.1 % of the 65 patients.

Table 3.2. The minimal overlapping regions of most common copy number losses detected by aCGH in 65 patients with endometrial cancer.

Chromosomal location	Start (bp)	Stop (bp)	Size (kB)	Patients with losses		Representative genes*
				Number	Percentage [%]	
Xp22.33	1047029	1106951	58.5	24	36.9	
17p13.1	7579476	7579877	0.4	17	26.1	*TP53*
15q11.2	25425129	25469275	43.1	17	26.1	
Xq28	152643761	152968889	317.5	16	24.6	*BGN*
16p13.3	2122529	2139286	16.4	16	24.6	*TSC2*
17p13.1	7572966	7573886	0.9	15	23.1	*TP53*
16q12.2	56370474	56374162	3.6	14	21.5	
9q34.3	139398117	139409336	11	15	23.1	*NOTCH1*
12q24.33	133218931	133220645	1.7	15	23.1	*POLE*
16q22.1	70169117	70195196	25.5	14	21.5	
4p16.3	1796047	1806500	10.2	14	21.5	*FGFR3*
19p13.3	291709	460661	165	14	21.5	
16p13.3	565954	1287835	705	13	20.0	*MSLN; SOX8*
16q24.2q24.3	88505908	88796498	283.8	13	20.0	*IL17C*

*Representative genes are the endometrial cancer related genes encompassed in the region.

Further step, we analyzed the most common imbalanced chromosomal band regions, aim to identify endometrial cancer with genomic imbalances. Specifically, we proposed a theoretical definition: with the presence of at least one imbalance region in one of the three most common regions, will be served as a confirmation of endometrial cancer. Figure 12 below represents the frequency of CNVs of the recruited 65 samples, the most three common minimal overlapping regions are 3p22.1 (41281477-41281777), 4q31.3 (153269677-153269977) and 5q22.2 (112164360-112164659), where the genes *CTNNB1*, *FBXW7* and *APC* located, respectively. Table 3.3 listed the copy number changes of each patient in above three regions. As it can be seen from the Table 3.3, there are 62 tumor samples with at least one aberration among three selected regions, where 20 patients have one imbalanced chromosomal band region, 13 patients have two imbalanced chromosomal band regions and 29

patients show aberrations in all three regions, only three tumor cases were found without aberrations in these regions. To obtain the sensitivity, which can correctly measure the proportion of actual endometrial cancer cases, and help correctly identify endometrial cancer, we used the following formula:

Quotient of true positive test results (cancer =copy number gain or loss) and the sum of true positive test results (cancer = copy number gain or loss) and false negative test results (also cancer, but copy number neutral in all three locations).

$$Sensitivity = \frac{true\ positive\ test\ results}{true\ posive\ test\ results + false\ negative\ test\ results} \times 100\ \%$$

$$Sensitivity = \frac{one\ aberration + \ two\ aberrations + three\ aberrations}{no\ aberration + one\ aberration + two\ aberrations + three\ aberrations} \times 100\ \%$$

$$Sensitivity = \frac{20 + \ 13 + 29}{3 + 20 + 13 + 29} \times 100\ \%$$

$$Sensitivity = 95.4\ \%$$

The higher the sensitivity of a test, the more reliable when it recognizes the illness. Which means that by combination of these three promising imbalanced regions, the sensitivity for identifying the endometrial cancer is really promising.

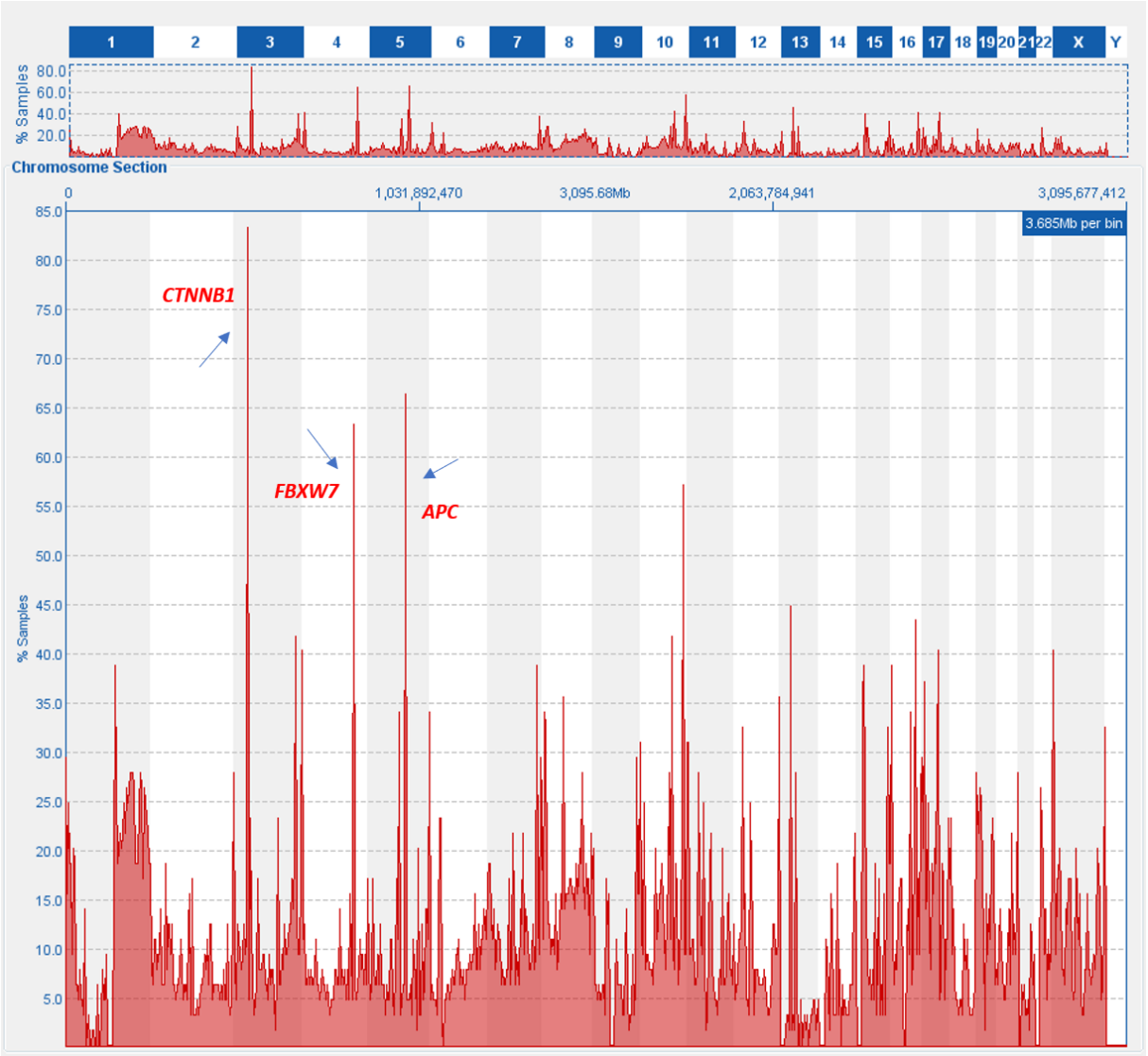

Figure 12. Overview of the frequency of copy number changes in 65 endometrial cancer patients. Arrows are the most common minimal overlapping regions and related genes.

Table 3.3. Copy number changes of three most common minimal overlapping regions in 65 endometrial cancer patients.

Chromosomal location	**3p22.1 (41281477-41281777)**	**5q22.2 (112164360-112164659)**	**4q31.3 (153269677-153269977)**
Related genes	***CTNNB1***	***APC***	***FBXW7***
Patients with CNV [%]	**84.6**	**66.2**	**64.6**
Case number		**Copy number changes**	
1	gain	gain	gain
2	gain	gain	gain
3	gain	gain	gain

Chromosomal local location	3p22.1 (41281477-41281777)	5q22.2 (112164360-112164659)	4q31.3 (153269677-153269977)
4	gain	gain	Gain
5	gain	gain	gain
6	gain	gain	gain
7	gain	gain	gain
8	gain	gain	gain
9	neutral	neutral	neutral
10	gain	neutral	neutral
11	neutral	gain	neutral
12	gain	neutral	gain
13	gain	neutral	neutral
14	neutral	neutral	gain
15	gain	gain	neutral
16	gain	neutral	gain
17	gain	gain	gain
18	gain	gain	gain
19	gain	neutral	gain
20	neutral	gain	gain
21	gain	gain	gain
22	gain	gain	neutral
23	gain	neutral	neutral
24	gain	neutral	neutral
25	gain	gain	gain
26	gain	gain	gain
27	gain	neutral	neutral
28	gain	neutral	neutral

Chromosomal local location	3p22.1 (41281477-41281777)	5q22.2 (112164360-112164659)	4q31.3 (153269677-153269977)
29	gain	gain	Gain
30	gain	gain	gain
31	gain	gain	neutral
32	gain	gain	gain
33	gain	gain	gain
34	gain	gain	gain
35	gain	neutral	neutral
36	gain	gain	gain
37	gain	neutral	gain
38	gain	neutral	neutral
39	gain	gain	gain
40	gain	neutral	gain
41	gain	gain	gain
42	gain	gain	gain
43	gain	neutral	gain
44	gain	gain	gain
45	gain	gain	gain
46	gain	gain	neutral
47	neutral	gain	gain
48	neutral	neutral	neutral
49	loss	neutral	neutral
50	gain	gain	gain
51	neutral	neutral	neutral
52	neutral	gain	gain
53	gain	gain	gain

Chromosomal local location	3p22.1 (41281477-41281777)	5q22.2 (112164360-112164659)	4q31.3 (153269677-153269977)
54	neutral	gain	Neutral
55	gain	neutral	gain
56	gain	gain	neutral
57	gain	gain	gain
58	gain	gain	gain
59	gain	gain	neutral
60	gain	neutral	gain
61	gain	neutral	neutral
62	neutral	gain	gain
63	gain	gain	gain
64	gain	loss	neutral
65	loss	gain	neutral

Figure 13. CTNNB1, FBXW7 and APC genes are located within the three genomic regions showing the most frequent gains and losses in 65 endometrial cancers analyzed in this study.

3.2. Distinguish between type I and type II endometrial cancer

Endometrial cancers are typically designed as type I and type II tumors. Type I tumors are more commonly develop in premenopausal or perimenopausal women and mostly low-grade (G1 or G2) tumors. They are normally diagnosed at an early stage before extra-uterine spread, and therefore, often have a relatively favorable prognosis. In contrast, type II endometrial cancers tend to develop in postmenopausal, non-obese women, it is normally poorly differentiated high-grade tumor and associated with higher risk of metastasis and poor prognosis. As there are big different in pathogenesis between two types, it is important to accurate classification, which could play an important role in patients' treatment and prognosis. To determine whether it is possible to distinguish the two endometrial cancer types through array-based CNVs, the most common overlapping abnormal regions were classified and analyzed based on two different types. Figure 14 illustrates the proportion of most common overlapping copy number gain regions in two different types of endometrial cancer. The most common copy number gain regions in both groups are the same, 3p22.1 (41281477-41281777), 4q31.3 (153269677-153269977) and 5q22.2 (112164360-112164659). More than 30 % of Type I cases were

gained at all listed chromosomal band regions, except 3q26.32 (178937437-178937736) and 15q26.1 (93428882-93435270), which were gained in 28.6 % of type I cases. In type II group, 13q13.1 (32950650-32950950) were gained in 17.4 % of patients, 16q22.3 (73092864-73093164) were gained in 21.7 % of patients and 26.1 % of patients were gained at 5q15 (92922322-92922819), rest of the listed regions are all gained in more than 30 % of type II endometrial cancer patients. Only 13q13.1 (32950650-32950950) were statistically significant between two groups (p<0.05).

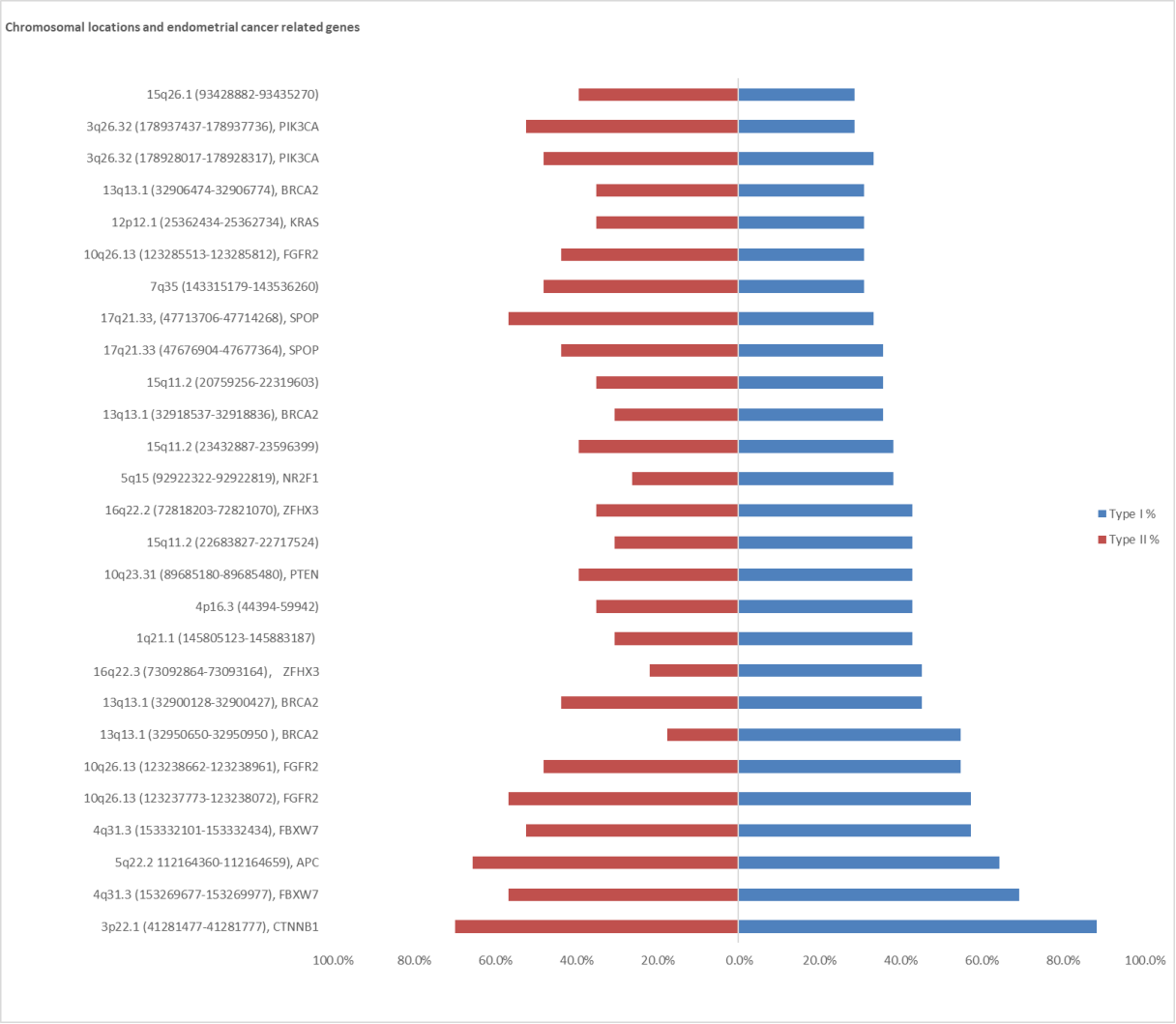

Figure 14. The minimal overlapping regions of most common copy number gains in two different types of endometrial cancers.

Figure 15 shows the proportion of most common overlapping copy number loss regions in two different types of endometrial cancer. As shown in Figure 15, 38.1 % of type I patients were lost at Xp22.33 (1047029-1106951), less than 20 % of type I patients were lost at rest of the most common chromosomal band regions. In type II group, 26.1 % of patients were lost at 16p13.3 (565954-1287835) and 16q24.2q24.3 (88505908-88796498), rest of the chromosomal band regions were lost in more than 30 % of type II patients. No significant differences between the two groups were evident (p>0.05).

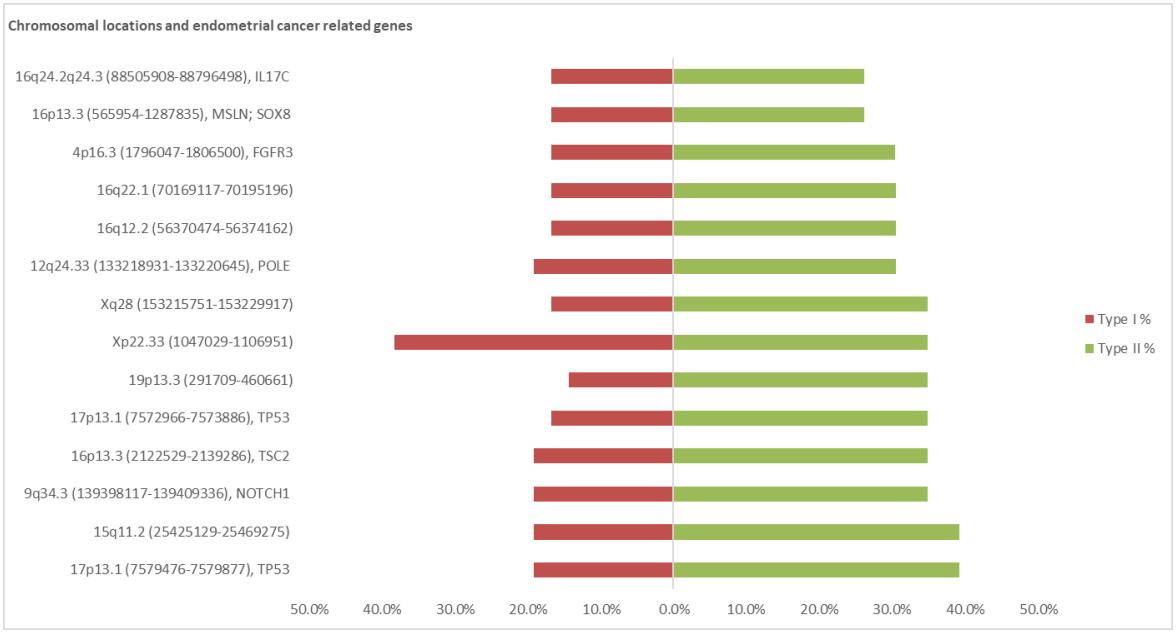

Figure 15. The minimal overlapping regions of most common copy number losses in two different types of endometrial cancers.

Clearly, by comparing the most common copy number gains and losses between two groups are not sufficient to distinguish the two endometrial cancer types. To further analysis, a criterion to look for the significantly aberrant regions was established:

1. Areas with the most different number of aberrations in cases of both classes
2. One class must account for more than 30 % of cases

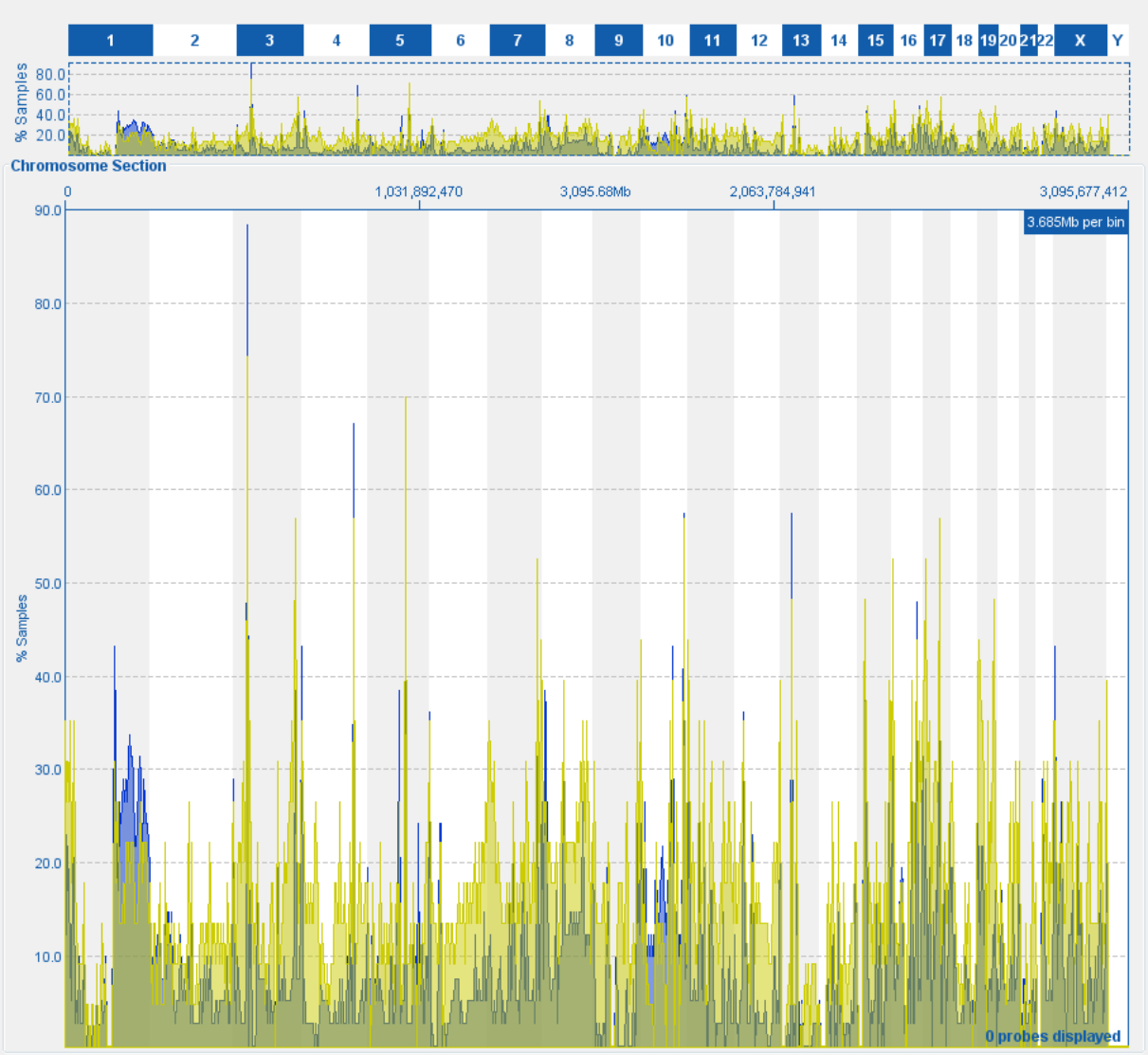

Figure 16. The frequency of CNVs compared in two different groups. Blue indicates type I, light yellow represents type II cases and light blue regions indicate the overlapping area of the two types.

Table 3.4. The most significantly imbalanced regions which could differentiate between two types.

Chromosomal location	Start (bp)	Stop (bp)	Aberrations-type I		Aberrations-type II		*p*-value
			Number	Percentage [%]	Number	Percentage [%]	
16q22.1	67937732	68100313	0	0	7	30.4	0.0002
17q21.32	46062980	46159303	0	0	7	30.4	0.0002
22q12.2	30098053	30126722	2	4.8	7	30.4	0.0042
1p36.11	27879864	27884157	1	2.4	8	34.8	0.0003

Chromosomal location	Start (bp)	Stop (bp)	Aberrations-type I		Aberrations-type II		*p*-value
			Number	Percentage [%]	Number	Percentage [%]	
Xp22.33	305511	316464	3	7.1	8	34.8	0.0045
1p36.32	2722682	2788698	4	9.5	8	34.8	0.0121
19p13.3	6060066	6303724	4	9.5	8	34.8	0.0121
19q13.32	46267865	46287563	4	9.5	11	47.8	0.0005
20q13.2	52106616	52128270	1	2.4	7	30.4	0.001
20q13.2	52234495	52265011	1	2.4	7	30.4	0.001
7p21.1	16663156	17270949	1	2.4	8	34.8	0.0003
7p22.3	1531412	1635547	3	7.1	8	34.8	0.0045
1p36.33	1024155	1150571	5	11.9	8	34.8	0.0275
19p13.3	2068056	2533713	5	11.9	10	43.8	0.0039
7q31.1	110404154	111065282	2	4.8	7	30.4	0.0042
3q26.1	167454903	167467350	2	4.8	8	34.8	0.0013
19q12	30435443	30496101	2	4.8	8	34.8	0.0013
7p22.3	1981050	2071279	4	9.5	8	34.8	0.0121
11p13	31828251	31831554	4	9.5	8	34.8	0.0121
13q13.1	32950650	32950950	24	57.1	4	17.4	0.002

Figure 16 displays a whole overview of the CNVs frequency in two different types. In Table 3.4 is shown the data from the summarized imbalanced regions. In total of 20 abnormal regions differentiated significantly between two types ($p<0.05$). To increase the sensitivity of distinguish between two types, the two sensitive regions with the largest differences between two subgroups were combined, 16q22.1 (67937732-68100313) with no type I and 30.4 % type II, 13q13.1 (32950650-32950950) with 57.1 % type I and 17.4 % type II. In order to maximize the effectivity of this combination for successfully distinguish between two different types, the data were assessed by using the criteria mentioned below (Table 3.5).

Table 3.5. Interpretation logic to distinguish between two endometrial cancer types.

Imbalanced region	Aberration-type I	Balanced-type I	Aberration-type II	Balanced-type II
Chr16q22.1	Type I= no	Type I= yes	Type II= yes	Type II= no
Chr13q13.1	Type I= yes	Type I= no	Type II= no	Type II= yes

Table 3.6 exhibits the aberration status of each endometrial cancer patient. 25 cases (38.5 %) could be correctly identified as type I and 7 cases (10.8 %) could be correctly identified as type II. However, 4 type II cases (6.2 %) would be misidentified as type I and 29 cases (44.6 %) could not be classified by using this interpretation logic. Closer examination of 55.4 % of endometrial cancer cases, which could be classified using our interpretation logic, the sensitivity of correct classification was then calculated as follows:

$$Sensitivity\left(type\ {}^{I}/_{II}\right) = \frac{correctly\ classified\ samples}{correctly\ classified\ samples + indetermined\ samples + misidentified\ samples} \times 100\%$$

$$Sensitivity = \frac{25 + 7}{(25 + 7) + 29 + 4} \times 100\ \%$$

$$Sensitivity = 49.2\ \%$$

Table 3.6. The aberration status of two sensitive regions with the largest differences between two types in 65 endometrial cancer cases.

Case number	Histological type	16q22.1 (67937732-68100313)	13q13.1 (32950669-32950968)	Interpretation logic
1	1	no	no	indetermined
2	1	no	gain	classified as type I
3	1	no	gain	classified as type I
4	1	no	no	indetermined
5	1	no	gain	classified as type I
6	1	no	gain/LOH	classified as type I
7	1	no	gain	classified as type I
8	1	no	gain	classified as type I
9	1	no	no	indetermined
10	1	no	no	indetermined
11	1	no	no	indetermined
12	1	no	gain	classified as type I
13	1	no	gain	classified as type I
14	1	no	no	indetermined
15	1	no	gain	classified as type I

Case number	Histological type	16q22.1 (67937732-68100313)	13q13.1 (32950669-32950968)	Interpretation logic
16	1	no	no	indetermined
17	1	no	gain	classified as type I
18	1	no	no	indetermined
19	1	no	no	indetermined
20	1	no	gain	classified as type I
21	1	no	gain	classified as type I
22	1	no	gain	classified as type I
23	1	no	no	indetermined
24	1	no	no	indetermined
25	1	no	gain	classified as type I
26	1	no	gain	classified as type I
27	1	no	no	indetermined
28	1	no	no	indetermined
29	1	no	gain	classified as type I
30	1	no	no	indetermined
31	1	no	gain	classified as type I
32	1	no	no	indetermined
33	1	no	gain	classified as type I
34	1	no	gain	classified as type I
35	1	no	loss	classified as type I
36	1	no	gain	classified as type I
37	1	no	gain	classified as type I
38	1	no	gain	classified as type I
39	1	no	no	indetermined
40	1	no	gain	classified as type I
41	1	no	no	indetermined
42	1	no	gain	classified as type I
43	2	no	gain	classified as type I
44	2	no	no	indetermined
45	2	no	no	indetermined
46	2	no	no	indetermined
47	2	no	no	indetermined
48	2	no	no	indetermined
49	2	loss	no	classified as type II

Case number	Histological type	16q22.1 (67937732-68100313)	13q13.1 (32950669-32950968)	Interpretation logic
50	2	no	no	indetermined
51	2	no	no	indetermined
52	2	no	no	indetermined
53	2	loss	no	classified as type II
54	2	no	no	indetermined
55	2	no	no	indetermined
56	2	no	no	indetermined
57	2	loss	no	classified as type II
58	2	loss	no	classified as type II
59	2	loss	no	classified as type II
60	2	loss	no	classified as type II
61	2	loss	no	classified as type II
62	2	no	gain	classified as type I
63	2	no	gain	classified as type I
64	2	no	no	indetermined
65	2	no	gain	classified as type I

3.3. Loss of heterozygosity

LOH is a common phenomenon in a variety of human cancers. As previously described, LOH is thought to contribute to localize tumor suppressor genes. Examining the link between LOH and endometrial cancer may help us identify tumor suppressor genes which are associated with endometrial cancer. There are 22 (33.8 %) of samples exhibited LOH, in which 11 (26.2 %) type I and 11 (47.8 %) type II tumors. Figure 17 below displays the overview of the whole LOH regions of these 22 endometrial cancer samples, LOH aberrations were distributed throughout all the autosomes and the X chromosome, except for chromosome 19-22. At least three cases showed LOH at Table 3.7 listed regions, the related genes and copy number aberrations of these cases are also displayed in the table. From this data, we can see that at 4 cases were observed LOH at 17q12q21.2, at 4p15.2p15.1 and 12q24.13q24.22 LOH were observed only in type II cases, and LOH at 10q22.2q22.3 and 10q25.2q26.11 were showed only in type I cases.

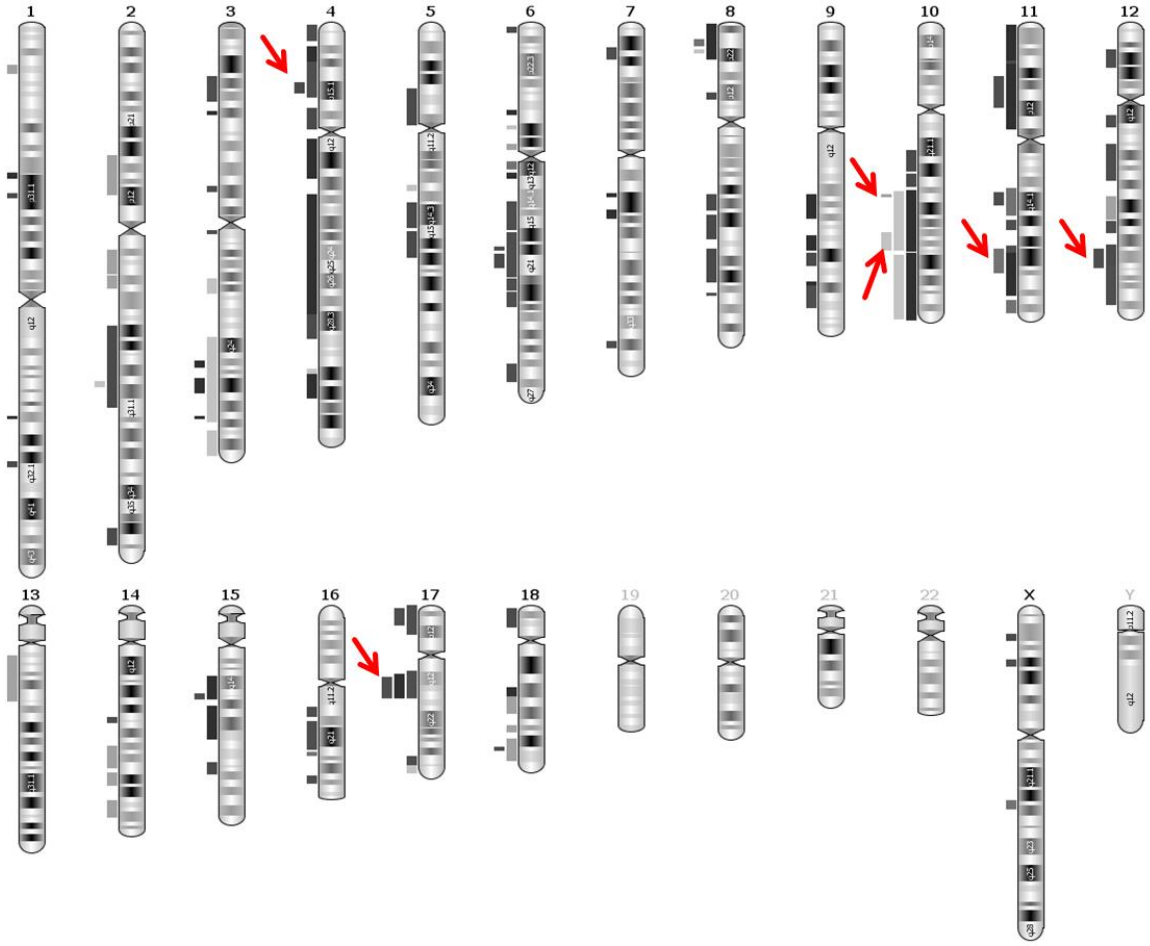

Figure 17. Loss of heterozygosity profiles of 22 endometrial cancer patients. Each columnized line denotes a single sample, red arrow indicates most overlapping LOH regions.

Table 3.7.Copy number changes of minimal most common overlapping LOH regions in 22 endometrial cancers.

Chromosomal location	Start	Stop	Case No.	Type	Copy number
4p15.2p15.1	27571339	29799673	46	II	loss
			61	II	loss
			57	II	gain
10q22.2q22.3	77550153	78805067	24	I	gain
			18	I	gain
			25	I	neutral
10q25.2q26.11	112922379	119602345	25	I	neutral
			3	I	neutral
			24	I	gain
11q22.3q23.2	103957598	112794247	46	II	loss
			61	II	loss
			21	I	neutral
12q24.13q24.22	113748561	117975814	49	II	neutral
			61	II	loss
			57	II	gain
17q12q21.2	36032814	38904276	61	II	loss
			53	II	gain/loss
			46	II	loss
			9	I	neutral

DNA double-strand-breaks can be repaired by homologous recombination (HR) pathway (Shrivastav et al. 2008). Defects in HR repair related genes can lead to HR deficiency. Genomic scars as biomarkers of HR deficiency, can be observed by large-scale state transitions (LST), telomeric allelic imbalance (TAI) and LOH (Watkins et al. 2014). To investigate the possible role of HR deficiency in endometrial cancer, we also looked into the LOH status of HR related genes: *ARID1A, ATM, ATRX, BAP1, BARD1, BLM, BRCA1/2, BRIP1, CHEK1/2, FANCA/C/D2/E/F/G/L, MRE11A, NBN, PALB2, RAD50, RAD51, RAD51B, or WRN* (Musacchio et al. 2020). In our cancer samples, LOH were observed at gene loci *ATM*, *BRCA1/2, RAD51, RAD51B, CHEK1, NBN* and *FANCC,* rest of the genes didn't show LOH (Table 3.8*)*.

Table 3.8. Copy number status of HR related genes with LOH in 22 endometrial cancer.

HR related genes	Case Number	Type	Copy number change
ATM	46	II	loss
	65	II	loss
BRCA1	46	II	loss
	61	II	loss
	53	II	loss
BRCA2	6	I	gain
RAD51	46	II	loss
RAD51B	15	I	neutral
CHEK1	21	I	neutral
NBN	57	II	neutral
FANCC	46	II	loss

Furthermore, we looked into the LOH status of most common aberrated regions, we can see from the Table 3.9 below, 7 most common minimal overlapping chromosomal band regions showed LOH.

Table 3.9. Most common CNV regions with LOH.

Chromosomal location	Start	Stop	Related gene	Case No.	Type	CNV
3p22.1	41281477	41281777	*CTNNB1*	22	I	gain
3q26.32	178937437	178937736	*PIK3CA*	24	I	gain
4p16.3	1796047	1806500	*FGFR3*	61	II	loss
10q23.31	89685180	89685480	*PTEN*	25	I	gain
13q13.1	32950650	32950950	*BRCA2*	6	I	gain
16q12.2	56370474	56374162		61	II	loss
17p13.1	7572966	7573886	*TP53*	61	II	loss

3.4. Microsatellite instability

Microsatellite instability is a molecular tumor phenotype resulting from genomic hypermutability. MMR system corrects spontaneous mutations in repetitive DNA sequence. It can result in MSI, when MMR system arises impairments. MSI is relatively common in endometrial cancer and is a potential marker for molecular classification and treatment of endometrial cancer. Therefore, microsatellite

instability was investigated in our tumor samples. Fifty-six cases were tested with Promega MSI analysis system, 9 cases were ruled out due to lack of corresponding normal tissue. MSI was identified in 14/56 cases (25 %), in which 9 cases of type I and 5 cases of type II endometrial cancers, no significant differences were found between the two histological types (p>0.05) Table 3.10.

Table 3.10: Statistical analysis of microsatellite status of 56 tested endometrial cancer cases.

Microsatellite status	Type I cases	Type II cases	*p*-value
instable	9	5	0.26
stable	27	15	0.26

3.5. Molecular classification includes LOH by aCGH

In 2018 our group presented a classification scheme to assign endometrial cancer to one of the four molecularly classified subgroups which proposed by TCGA study (Weimer et al. 2018; Kandoth et al. 2013). This cluster analysis was performed based on a combination of aCGH, microsatellite status and histological type information. The first step in this process was to assess microsatellite instability. By testing, when the samples tested MSI, they would be classified into the MSI group. The remaining MSS cases were then evaluated based on CNVs, LOH and histological type. Type II cases that were aberrated in gene locus *TP53* would be classified as serous like/*TP53* group. *POLE* group was then defined when aberrations in *POLE* gene locus appeared. Finally, the rest of the MSS cases were classified as MSS group, the cases without microsatellite status would remain unclassified (Figure 18).

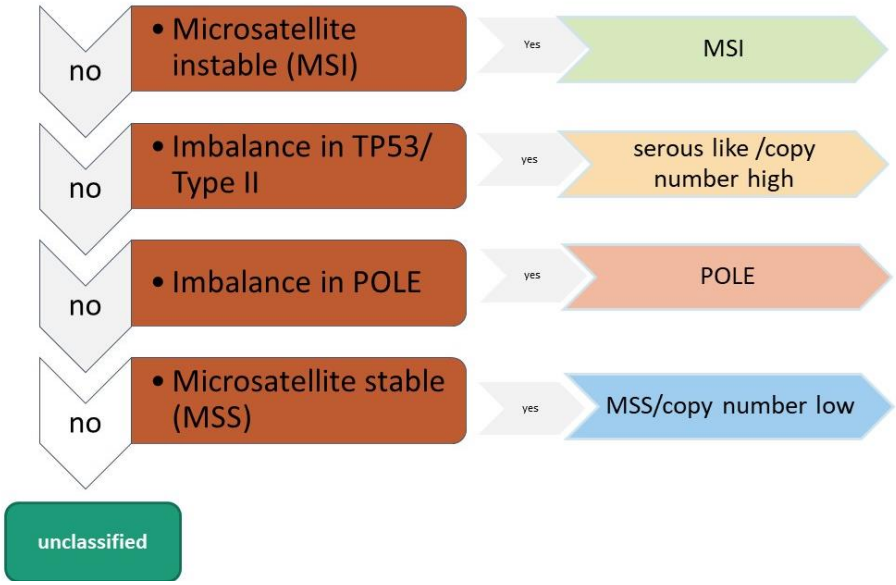

Figure 18: Classification scheme for endometrial cancer in combination of histology, aCGH and MSI-test analysis.

Table 3.11 shows the results of classification of all 56 endometrial cancer cases by the above classification scheme, tumor samples are classified into four distinct subgroups using our above-mentioned algorithm. Due to the lack of microsatellite instability information, 9 samples are unclassifiable. Among the tested samples, 14 cases (25 %) classified as MSI group, 11 cases (19.6 %) as serous like group, 17 samples (30.4 %) as *POLE* group and 14 cases (25 %) as MSS group. Interestingly, although the classification of *POLE* group was not based on the histological type, 94 % of our samples in this group were type I cancer. With help of high-resolution array, we were able to identify the CNVs in the interesting genes loci. As listed in the Table 3.11 below, the incidence of CNVs in related gene loci is different among the four subgroups.

Table 3.11. Classification of endometrial cancer according to histology, aCGH and microsatellite instability analysis.

	MSI	**serous-like/*TP53***	***POLE***	**MSS**
Number of samples	25 %	19.6 %	30.4 %	25 %
Microsatellite status	MSI	MSS	MSS	MSS
Type I	64 %	0	94 %	71 %
Type II	36 %	100 %	6 %	29 %
Frequency of CNVs identified in gene loci	*FBXW7* (86 %)	*TP53* (100 %)	*POLE* (100 %)	*FGFR2* (100 %)
	BRCA2 (79 %)	*APC* (100 %)	*CTNNB1* (100 %)	*FBXW7* (100 %)
	CTNNB1 (79 %)	*FGFR2* (100 %)	*FGFR2* (94 %)	*CTNNB1* (93 %)
	FGFR2 (79 %)	*SPOP* (100 %)	*BRCA2* (88 %)	*APC* (86 %)
	APC (71 %)	*BRCA2* (91 %)	*SPOP* (88 %)	*BRCA2* (79 %)
	POLE (64 %)	*KRAS* (82 %)	*FBXW7* (82 %)	*PTEN* (50 %)
	PTEN (64 %)	*ZFHX3* (91 %)	*PTEN* (71 %)	*PIK3CA* (57 %)
	PIK3CA (64 %)	*CTNNB1* (91 %)	*PIK3CA* (77 %)	*SPOP* (36 %)
	SPOP (64 %)	*FBXW7* (91 %)	*KRAS* (71 %)	*KRAS* (36 %)
	KRAS (64 %)	*PIK3CA* (82 %)	*ZFHX3* (77 %)	*CSMD3* (21 %)
	TP53 (57 %)	*POLE* (82 %)	*APC* (71 %)	*TP53* (21 %)
	ZFHX3 (50 %)	*PTEN* (73 %)	*TP53* (59 %)	
	ARID1A (36 %)	*ARID1A* (64 %)	*ARID1A* (41 %)	
	RPL22 (29 %)	*CSMD3* (27 %)	*CSMD3* (24 %)	
	CSMD3 (14 %)	*RPL22* (27 %)	*APOB* (24 %)	
	CCNB3 (14 %)	*ABCA5* (18 %)		

Furthermore, the number of CNVs in all tested cases were summarized. We focused on the four categories of cases that were classified by our criteria and plotted to observe the differences of CNVs among the four subgroups (Figure 19). The number of CNVs in the MSI group ranged from 22 to 505 with a median of 56.6, in serous like/ *TP53* group was between 75 and 335, with a median of 143. In the *POLE* group, the number of CNVs was between 29 and 454, with a median of 68, in the MSS group, it ranged from 24 to 140 with a median of 37. Welch t-test (unpaired t-test with unequal variance) was used to compare the CNVs between four subgroups. Stratifying the CNVs by endometrial cancer subtypes revealed considerable differences, with the highest fraction of CNVs for the serous like/*TP53* group (mean=174, p=0.041) and the lowest fraction for the MSS group (mean=47, p=2.42×10^{-5}). The fraction of CNVs in POLE group and MSI group didn't show significantly differences in compare with other subtypes. The distribution of CNVs, especially in serous like and MSS group, are in line with Hong's molecular classification.

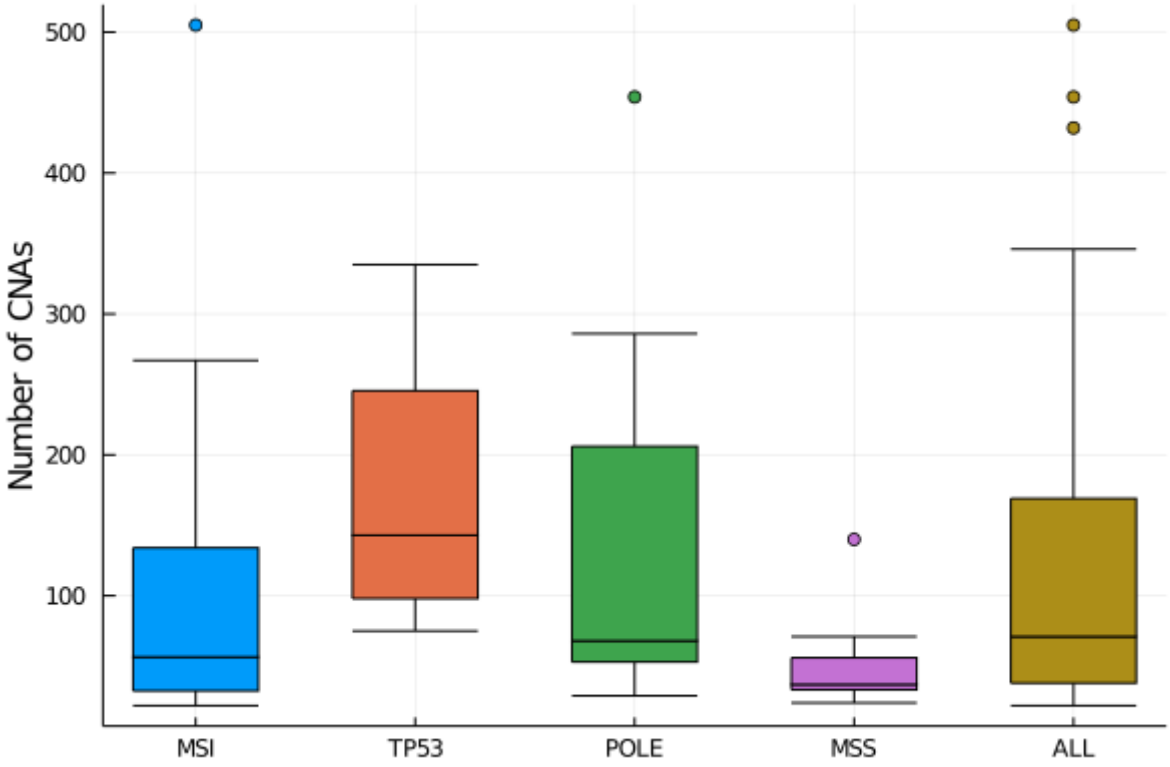

Figure 19. Comparison of copy number variations of across the four endometrial cancer subgroups. The box plot represents the median (thick lines) and the range of CNVs (boxes). The distance between the upper and lower horizontal black lines (upper and lower whiskers) and the 75th and 25th percentiles is 1.5 times the interquartile range. Whereas serous like/*TP53* group harbored the highest levels of CNVs (p = 0.041, unpaired t test with unequal variance, testing for differences between the serous like/*TP53* subtype and all other three subtypes), tumors of the MSS group displayed the lowest fraction of CNVs (p = 2.42×10^{-5}, unpaired t test with unequal variance, testing for differences between MSS subtype and all other three subtypes). *POLE* group and MSI group didn't show significantly differences in compare with other subtypes.

4 Discussion

4.1. Copy number variation

Most malignant tumors are characterized by chromosomal alterations, like CNVs. Therefore, identify and understand CNVs could also be regarded as potential biomarkers, which may provide a considerable opportunity for a patient's diagnosis, prognosis, and refinement of further treatment. Thus far, previous studies have attempted to evaluate the impact of CNVs in endometrial cancer. A CGH analysis of 43 endometrial cancer samples revealed copy number gains at 1q25-q41 (23 %), 8q11.1-q21.1 (23 %), and 8q21.3-qter (21 %) (Hirasawa et al. 2003). In comparison, copy number gains were observed in 27.7 %, 35.4 % and 27.7 % of our 65 endometrial cancer patients at 1q25-q41, 8q11.1-q21.1 and 8q21.3-qter, respectively. A series of genome wide association study in European populations have identified 16 endometrial cancer genetic risk regions: 1p34.3, 2p16.1, 6q22.3, 6q22.31, 8q24.21, 9q21.3, 11p13, 12p12.1, 12q24.12, 12q24.21, 13q22.1, 15q15.1, 15q21.2, 17q11.2, 17q12 and 17q21.32 (O'Mara et al. 2019), all of these CNVs have also been occasionally found in our tested endometrial cancer samples except 1p34.3. Almost 85 % of our endometrial cancer samples presented CNVs at chromosome regions 3p22.1, where the oncogene *CTNNB1* is located. Around 65 % of cases harbored CNVs at 5q22.1 and 4q31.3, where tumor suppressor genes *APC* and *FBXW7* are located, respectively. These three genes have been reported to be frequently mutated in endometrial cancer (Kandoth et al. 2013). With the information in which genomic regions the most common imbalances occur, FISH probes can be generated and used as biomarkers. While examining our data, we found that the smallest overlapping regions we observed were restricted to a size of 300 bp, making them too small for detection using FISH. Figure 13 shows in the very tiny CNV peaks many cases that exclusively have 300 bp in extent, which cannot be detected with FISH. The figure also shows CNVs in all three loci, which extend over larger areas that can certainly be detected with FISH. Thus, the combination of these three loci increases the probability of detecting a FISH signal pattern in endometrial cancer cells that deviates from the diploid pattern. The basis for this increased detection of non-diploid patterns is the accumulation of CNVs in endometrial cancers, detected here with aCGH, which reflects typical chromothripsis.

The study's findings suggest the potential development of a 3-Color FISH probe for diagnosing endometrial cancer by targeting three specific regions. This could lead to a FISH panel for identifying endometrial cancer. Moreover, the FISH technique can be applied to cells collected through vaginal smears, offering a noninvasive diagnostic possibility. However, it's essential to emphasize that the proposed diagnostic method requires further validation through randomized controlled trials to establish a reliable algorithm for identifying potential cancer patients. While the study shows promise, further work is required to confirm its clinical usefulness.

Type II endometrial cancers are typically more aggressive than type I cancers and have a poorer prognosis. Although Type II endometrial cancers only represent less than 10 % of all cases, they account for a disproportionate number of deaths from endometrial cancer. Therefore, we deliberately increased the proportion of type II endometrial cancers up to 35 % in our cohort in order to reduce the bias caused by a small sample size. Accurate pathological assessment of histology and tumor grade is essential for the patient management, because these classifications play big rule in determining the therapy and patient prognosis, all of which will used to direct surgery and adjuvant treatment. However, a histopathological misclassification in grade assignment, especially in high-grade endometrial cancers and also histologically misclassified cases have already been reported (Clarke and Gilks 2010; Kim et al. 2013; Kandoth et al. 2013). So far, very little research has been carried out on classifying endometrial cancer by array-based CNVs. Integrated assessment may be help identify histologically misclassified cases, with this aim, we approached to classify endometrial cancer by assessing the difference of CNVs between two types. Combining of 16q22.1 (67937732-68100313) and 13q13.1 (32950650-32950950), around half of our tumor samples can be divided into two subgroups (sensitivity 49.2 %). The sensitivity of correctly distinguishing between two types is relatively low, with the limited sample size, the findings might not be reassured.

4.2. Loss of heterozygosity

LOH has been used to localize tumor suppressor genes and is seen in 33.8 % of our samples. The most common regions are 4p15.2p15.1, 10q22.2q22.3, 10q25.2q26.11, 11q22.3q23.2, 12q24.13q24.22 and 17q12q21.2, suggesting that tumor suppressor genes located within these regions might be involved in the initiation and progression of endometrial cancer. LOH at 4p15.2p15.1 has been reported at other types solid tumors before, including cervical cancer and colorectal cancer, which indicates the possibility of multiple putative tumor suppressor genes located in this region (Shivapurkar et al. 2001; Sherwood et al. 2000). Tumor suppressor genes *PTEN, ATM, BRCA1* located at 10q, 11q and 17q, respectively. Mutations on these genes have been verified in endometrial cancer (Hong et al. 2015). We found three cases with copy number loss at *BRCA1 locus* and two cases with copy number loss at *ATM* gene locus, these under expressed genes may influence tumorigenesis through haploinsufficiency (Ryland et al. 2015). We found one copy number gain LOH at *PTEN* gene locus. LOH occurs at a gene locus as loss of one functional tumor suppressor gene allele and leaves only non-functional allele of the tumor suppressor gene. Copy number gain can duplicate the remaining allele and result in multiple non-functional tumor suppressor gene alleles, which may lead to the loss of function of tumor suppressor gene (Ching et al. 2011). This hypothesis provides some explanations of a link between gene copy number aberrations and loss of function. In further research, we can sequence these copy number gain LOH cases to verify this hypothesis.

Defects in homologous HR related genes can lead to HR deficiency, which can be detected by evaluating LST, TAI and LOH. Our result showed LOH in HR deficiency genes are more frequently in non-endometrioid cancer, which is in line with a previous publication (Jonge et al. 2019; Jönsson et al. 2021). LOH in *BRCA1* and *BRCA2* were observed in 1 type I case and 3 type II cases, respectively. Familial breast and ovarian cancers with *BRCA1* or *BRCA2* loss are highly sensitive to treatment with poly (ADP-ribose) polymerases (PARPs) inhibitors. Several studies demonstrated that HR deficiency in tumors could be a therapeutic target for PARPs inhibitors regardless of the *BRCA* mutational status (Turner et al. 2004; Dizdar et al. 2015). Given that PARP inhibitors targeted HR deficiency, endometrial cancers in patients with HR deficiency may benefit from these HR-targeted therapies. Recently, small size studies on PARP inhibitors targeting HR deficiency in *Tp53* mutated group showed promising results (Musacchio et al. 2020). Clearly, additional studies are needed with focus on HR deficiency in endometrial cancers and resolve the therapeutic value of PARPs in endometrial cancers.

4.3. Biomarker genes

CNVs has a positive linear effect on gene expression for the majority of genes (Shao et al. 2019). Copy number gain could increase the gene dosage and level of expression. Gain-of-function mutation are often generated by gene overexpression (Alberts B, Johnson A et al 2002). Thus, copy number gains in oncogenes could lead to the tumorigenesis. 84.6 % (55/65) of the tumors in our data showed imbalances at *CTNNB1 gene loci*, most of which are copy number gains. *CTNNB1* gene is an oncogene that encodes β-catenin and plays an essential rule in activation of Wnt/β-catenin signaling pathway. In previous reports by others, the gain-of -function of *CTNNB1* gene in endometrial cancer has been linked to nuclear accumulation of β-catenin and *CTNNB1* mutation (Inomata et al. 1996; Nei et al. 1999; Machin et al. 2002; Wang et al. 2017; Kurnit et al. 2017). Nuclear β-catenin expression is associated with *CTNNB1* exon 3 mutations (Moreno-Bueno et al. 2002). The publication of the TCGA endometrial cancer data suggests that tumors with *CTNNB1* mutation were predominantly contained within the MSS and copy number low endometrioid cluster (Hong et al. 2015). Several studies have identified that *CTNNB1* exon 3 mutation is implicated in aggressive subset of low-grade and low-stage endometrioid endometrial carcinoma (Liu et al. 2014; Myers et al. 2014; Kurnit et al. 2017). Comparison of our findings with those of other studies suggests that copy number gains and mutations in *CTNNB1* may complement each other in gain-of-function mutation.

CNVs were observed in 66.2 % (43/65) of our tumor samples at *APC* gene locus 5q22.1, where only one sample (2.3 %) harbored copy number loss. *APC* gene is a tumor suppressor gene, its protein regulates β-catenin levels by cooperating with kinase glycogen synthase kinase-3 β (GSK-3 β) via phosphorylation of multiple serine/threonine residues coded on β-catenin and induces the Wnt/β-catenin signaling pathway (Im Barth et al. 1997; Chan et al. 2012). *APC* mutations are reported in around 64 % of

colorectal cancers and 14 % of endometrial cancers (TCGA Pan Cancer Atlas). Since loss-of-function is the typical mechanism of tumor suppressor genes, copy number loss in *APC* should reduce gene dosage and lead to insufficient active protein for normal function, which contribute to tumorigenesis. Prior study noted that *APC* haploinsufficiency can be responsible for familial adenomatous polyposis with gene deletion being a possible cause of reduced gene expression (Venesio et al. 2003). The *APC* three-hit hypothesis proposed that colorectal cancers can respond by regulating Wnt/β-catenin signaling pathway through CNVs (Segditsas et al. 2009). This hypothesis may can also explain the rule of copy number gains in *APC* gene in endometrial cancer. *APC* and *CTNNB1* genes are promising in endometrial cancer because of their potential therapeutic relevance. They moderate the Wnt/β-catenin signaling cascade in different ways, which could be a rational approach for targeted therapeutics (Anastas and Moon 2013; Katoh and Katoh 2017; Krishnamurthy and Kurzrock 2018).

FBXW7, is a tumor suppressor involved in protein degradation. Numerous studies have suggested that inactivation or downregulation of *FBXW7* can lead to tumorigenesis (Sailo et al. 2019). In previous studies by others, lower expression of *FBXW7* in endometrial cancer and also in other types of cancers (breast cancer, gastric cancer etc.) have been reported (Sailo et al. 2019; Liu et al. 2020). *FBXW7* mutations are observed in 10 % endometrial cancers, in type II endometrial cancers the mutation rate is up to 22 % (Kuhn et al. 2012; Kandoth et al. 2013; Yeh et al. 2018). Yeh's studies have described that 47 % *FBXW7* mutant cells harbor *APC* gene mutation, but it is not yet clear whether these co-occurrences can accelerate cancer progression. In contrast to former reports, 64.6 % (42/65) of our tumor samples present copy number gains in *FBXW7* locus, which could increase *FBXW7* gene dosage and upregulate its function. CNV is a large segment of DNA in comparison with a reference genome, a CNV can encompass more than one gene, which in our case, the copy number gain in *FBXW7* could be an effect of other neighborhood genes.

ARID1A locus 1p36.11 showed CNVs in 35.4 % (23/65) of our endometrial cancer patients, two third of them are lost at this gene locus. *ARID1A,* a tumor suppressor involved in transcriptional regulation, it is a key member of the SWI/SNF chromatin-modeling complex and a potential biomarker in endometrial cancer. It has also been found that inhibition of the PI3K pathway contributes to the tumor-suppressor activity of *ARID1A* (Liang et al. 2012). Loss of *ARID1A* expression has been reported to be correlated with the *ARID1A* mutational status in gynecological cancers (Khalique et al. 2018). A recent study reported *ARID1A* expression is downregulated in Colorectal cancer tissues which correlates with it being a tumor suppressor protein (Erfani et al. 2020). Another study showed that uterine low-grade endometrioid carcinoma harbored high frequency of *ARID1A* mutations and frequent loss of *ARID1A* expression (Guan et al. 2011). In a classification of endometrial cancer, a 9 gene panel including *ARID1A*, *ARID1A* mutation was detected in 47 % of low-grade endometrioid adenocarcinomas, 60 % of high-grade endometrioid adenocarcinomas, 11 % of serous

adenocarcinomas, and 24 % of carcinosarcomas (McConechy et al. 2012). Interestingly, according to our classification scheme, there are no aberrations in the *ARID1A* gene locus in the MSS group. Unlike the TCGA classification, in which the *ARID1A* mutation was detected in all molecular classes except serous like group. These findings reflect differences in gene CNVs and mutations, further research should be undertaken to confirm our classification hypothesis.

There are 61.5 % (40/65) of our cases showed aberrations in chromosome 12q24.33, where the *POLE* gene is located. *POLE* encodes the catalytic subunit of DNA polymerase epsilon, an enzyme involved in DNA replication and repair. Since the loss-of-function is the typical mechanism that tumor suppressor genes involve in tumorigenesis, copy number loss in *POLE* gene may involve in initiation and progression of endometrial cancer. Among our *POLE* aberrated cases, 37.5 % (15/40) harbor copy number loss. *POLE* mutated tumors were identified as one of the four proposed molecular subgroups in TCGA classification. *POLE* mutations have been identified in 7-17 % endometrial cancer (Kandoth et al. 2013; López-Reig et al. 2019). Importantly, despite *POLE* mutated endometrial cancer shown a tight association with high histologic grade, it has a favorable prognostic when compared to other tumors of similar type, grade, and stage. (McConechy et al. 2016; Church et al. 2013). We classified 30.4 % (17/56) of our tumor samples as *POLE* group based on the aberration on *POLE* gene locus, which was much higher than TCGA classification scheme (7 %). 10.7 % (5/56) of our cases showed copy number loss in *POLE* gene in *POLE* group, which is more closer to the TCGA classification and also in consistent with previous reports (Kandoth et al. 2013; López-Reig et al. 2019). It is important to keep in mind our classification scheme is based on copy number aberrations, therefore, comparison with TCGA classification must be interpreted with caution. Furthermore, we deliberately increased the proportion of type II in our study, with a small sample size, these findings might not be reassured.

4.4. Microsatellite instability

The repair of DNA damage is a complex process that depends on particular pathways to remedy lesions to DNA. The MMR pathway is one of the excision pathways, which is able to repair single base mismatches and a variety of small insertions and deletions to the genome (Gavande et al. 2016). Microsatellites are short repeated sequences of DNA, they are prone to slippage or replication errors because of their repeat structure (Kanopiene et al. 2015). Usually, MMR system corrects errors that spontaneously occur during DNA replication. However, when MMR system is not functioning normally, it can result in MSI. MSI is relatively common in endometrial cancer, approximately 30 % of endometrial cancer cases indicated MSI (Bonneville et al. 2017; Kim et al. 2013). By comparison, 25 % of our tested samples with endometrial cancer included in our study presented MSI. In recent years MSI was intensively studied as a prognostic marker, but the role of MSI on outcomes in patients with endometrial cancer was controversial. Basil et al. report that MSI occurs in early stage of disease (Basil

et al. 2000). An et al. suggests that MSI represents poor prognostic (An et al. 2007). However, Kanopiene et al. found that there was no statistically significant relationship between MSI and survival of endometrial cancer patients (Kanopiene et al. 2015). Recent studies have shown that endometrial tumors with defective MMR/MSI high status might be excellent candidates for PD- 1 and PD-L1 check inhibitors. In an ongoing phase I/II study, PD-1 inhibitor dostarlimab showed an overall response rate of 49 % in MSI high advanced endometrial cancer versus 20 % in MSS tumors (Green et al. 2020; NCT03981796). A recent study on PD-1 antibody pembrolizumab included 49 unresectable or metastatic MMR- deficiency endometrial cancer patients showed an overall response rate of 57 % (Marabelle et al. 2020). The TCGA classification defined MSI as a new molecular subgroup and demonstrated the importance of MSI in endometrial cancer. Thus, we included the MSI testing in our research with the purpose of simulating the TCGA molecular classification using different algorithm. According to some studies, MSI is more common in endometrioid endometrial cancer (Kanopiene et al. 2015; An et al. 2007). However, in our test results, there was no significant difference in microsatellite status between the two main histological types (p>0.05). A possible explanation for this result may be the deliberate increase in the proportion of type II or the lack of adequate samples in our study.

4.5. Molecular classification of endometrial cancer

The TCGA network performed a landmark molecular study of 373 endometrial cancers and identified four major genomically defined subgroups, 7 % of cases were classified as *POLE*-mutated, 28 % were grouped as MSI, 39 % as MSS/copy-number-low and 26 % were identified as serous-like/copy-number-high group, these groups were also clinically significant and prognostic. This molecular classification presented a novel insight to interpret endometrial cancer. Subsequently, two research teams developed a simplified, low cost classification methodologies which could be applicable in routine diagnostic practice for identifying molecular subgroups of endometrial cancer (Talhouk et al. 2015; Stelloo et al. 2015; Stelloo et al. 2016; Talhouk et al. 2017). Talhouk's classification is also known as ProMisE (Proactive Molecular Risk Classifier for Endometrial Cancer) algorithm, which tested the surrogate markers of these molecular subgroups through immunohistochemistry for MMR proteins, sequencing with digital PCR to identify *POLE* exonuclease domain mutations (POLEEDM) and *TP53* immunohistochemistry. It classifies endometrial cancer as MMR-deficient subgroup, POLEEDM, p53wt (wild type) or p53abn (aberrant) and recapitulates the distinct prognostic outcomes observed in the TCGA subgroup classification. Similar to ProMisE, Stelloo et al. has identified four prognostic subgroups with potential therapeutic implications (Stelloo et al. 2016). *TP53* immunohistochemistry and sequencing of *TP53* mutations are combined to identify the *TP53* mutant subgroup; MSI was determined by Promega analysis system, immunohistochemistry for MMR proteins was performed as

supplemental test to identify the MSI subgroup, *POLE*-mutated group was then classified by means of sanger sequencing, the fourth group was then a group with no specific molecular profile. These pragmatic classification systems have established clinically applicable methodologies to assign endometrial cancers to different molecular subtypes with particular clinical outcomes.

Our custom-designed array was fitted with high resolution for 13 genes that described by TCGA (Table 2.2). It enables us to identify CNVs in these gene regions and provides us with genomic information from the perspective of cytogenetics. It has been established that genomic classes of endometrial cancer are associated with phenotypes. Thus, we attempt to design a simple classification algorithm in combination with aCGH, analysis of MSI and histology, which might also recapitulate the TCGA subtypes. 55 cases were analyzed and assigned to four distinct subtypes based on our classification scheme. We used Promega MSI analysis system to test MSI, 25 % cases were identified as MSI cluster. In the TCGA analysis, more than 90 % of cases were noted to be TP53 mutated in the copy-number high group and most of them were in serous histology. While clear cell carcinomas were not analyzed by TCGA, Dalair's study confirmed that most of the clear cell endometrial cancers are TP53 mutated and can be categorized into serous like group (DeLair et al. 2017). Afterwards, we assessed the CNVs in *TP53* gene locus using aCGH and combined with histology, classified 19.6 % of cases into serous like group. Following determination of MSI and serous like groups, we classified 30.4 % of cases as *POLE* group when imbalances were observed in *POLE* gene locus. Finally, 25 % of cases were defined as MSS group. In addition, CNVs in different subgroups were also observed (Figure 19), the CNVs distribution are consistent with TCGA classification. Serous like group and MSS group can also be described as copy-number-high group and as copy-number-low, respectively. While our molecular analysis is limited to aCGH, above findings indicate that our classification scheme could be a novel approach for classifying endometrial cancer. However, this classification system is the lack of clinical data support, of which could verify this approach by recapitulate the clinical prognosis. Clearly additional studies are needed to resolve any significant relationship between different subtypes and clinical relevance. Our *POLE* group (30.4 %) is considerably higher than the TCGA classification (7 %), aberrant of genes are much more in serous like group rather than *POLE* group, which are inconsistence with TCGA classification. These differences may partly be explained by the fact that aberrations in gene copy number is inconsistence with gene mutation. The fact that inadequate samples and artificially increased proportion of type II can also be the reason. Further studies are required to establish the viability of our classification. A possible area of future research would be done to reanalyze the above cases by NGS to confirm our classification algorithm.

Studies on the molecular characteristics of endometrial cancer have led to the identification of targetable molecular alterations in four subgroups and promoted genomic-guided therapy (Urick and Bell 2019). *POLE*-mutant and MSI subgroups are highly immunogenetic and with high concentrations

of tumor infiltrating lymphocytes, they have high PD-1 and PD-L1 expression and may benefit from PD-1/PD-L1 inhibitors. A clinical study on PD-1 blockade, which included 15 endometrial cancer patients, showed an objective radiographic responses rate of 53 % (Le et al. 2017). Mehnert et al. reported a *POLE*-mutant endometrial cancer patient experienced a prolonged response (>14 months) to anti-PD-1 therapy (Mehnert et al. 2016), further clinical trials specifically target *POLE* mutations with PD-1 antibody in endometrial and other cancers are in process (Mehnert 2020). Molecular-integrated risk stratification to determine the adjuvant therapy may reduce both under- and overtreatment of women with endometrial cancer. An ongoing PORTEC-4a trial leads by the Dutch Gynecologic Oncology Group is a randomized trial to implement the use of an integrated clinic-pathological and molecular risk profile to determine adjuvant treatment for endometrial cancer. In this trial, the four molecular subgroups are combined with other prognostic factors (L1-cell adhesion molecule expression, LVSI, *CTNNB1* mutation) to designate favorable, intermediate, and unfavorable profile with a significantly different recurrence-free survival (van den Heerik et al. 2020a; van den Heerik et al. 2020b). The molecular classification should help sort patients into different prognostic groups, with the consequences of better predicting evolution and better orienting the treatment. In the coming years, the molecular classification of endometrial cancer would be a prognostic factor and guide for the treatment decision and the practice of targeted therapy should improve patient outcomes.

5 Conclusion

Endometrial cancer, arising from the lining of the uterus, is the most common gynecologic malignancy in the developed countries. Prognosis varies based on the histologic subtype and other clinical pathologic features (stage, tumor grade, LVSI). However, the determination of histological subtype and grade is unreliable, particularly in high-grade tumors, misclassified cases have already been reported. Early diagnosis of the cancer is essential for the treatment and prognosis, but it is still a major challenge.

We identified three imbalanced regions using aCGH, 3p22.1 (41281477-41281777), 4q31.3 (153269677-153269977) and 5q22.2 (112164360-112164659). In combination of BAC clones to target these three regions, it is possible to develop a FISH panel to identify endometrial cancer. For further research endometrial cells will be collected through vaginal smears and analyzed by FISH panel to confirm the imbalances. This study should be carried out to establish the appropriate method for early diagnosis of endometrial cancer.

33.8 % of our endometrial cancer samples harbored LOH. The most common regions are 4p15.2p15.1, 10q22.2q22.3, 10q25.2q26.11, 11q22.3q23.2, 12q24.13q24.22 and 17q12q21.2, suggesting that tumor suppressor genes located within these regions might be involved in the pathogenesis of endometrial cancer. LOH in HR deficiency genes were observed in our cases including *BRCA1/BRCA2* genes, indicating the possibility of therapeutic target for PARPs inhibitors.

The correct determination of histological subtype is essential for the treatment and prognosis of the endometrial cancer, as type II endometrial cancer is a highly aggressive variant of cancer. Two imbalanced areas were identified to distinguish between two histological types, 16q22.1 (67937732-68100313) and 13q13.1 (32950650-32950950). Approximately half of the cases could be correctly classified. These findings could become a cytogenetic tool to aid in the accurate and reproducible diagnosis of endometrial carcinoma subtypes.

We identified CNVs in endometrial related oncogenes and tumor suppressor genes. Particularly, the rule of CNVs tumorigenesis in *CTNNB1*, *ARID1A* and *POLE* genes are consistence with other previous studies. We established a classification scheme in combination of histological type, array-based CNVs and microsatellite status to recapitulate the TCGA molecular classification of endometrial cancer. Compared with the TCGA classification, the distribution of CNVs in serous like group and MSS group are highly consistent. It is worth emphasizing that inadequate sample size and artificially increased type II proportion may be responsible for the different proportion of the cases compare with TCGA classification. This is an important issue for future research, it is worth pursuing further is to test all our tumor samples with NGS to confirm our classification algorithm.

6 Publication bibliography

Aarnio, M.; Sankila, R.; Pukkala, E.; Salovaara, R.; Aaltonen, L. A.; La Chapelle, A. de et al. (1999): Cancer risk in mutation carriers of DNA-mismatch-repair genes. *International journal of cancer* 81 (2), 214–218.

Alberts B, Johnson A et al (2002): Molecular Biology of the Cell. Studying Gene Expression and Function. New York: Garland Science. Available online at https://www.ncbi.nlm.nih.gov/books/NBK26818/.

Amant, F.; Mirza, M. R.; Koskas, M.; Creutzberg, C. L. (2018): Cancer of the corpus uteri. *International journal of gynaecology and obstetrics: the official organ of the International Federation of Gynaecology and Obstetrics* 143 Suppl 2, 37–50.

An, H. J.; Kim, K. I.; Kim, J. Y.; Shim, J. Y.; Kang, H.; Kim, T. H. et al. (2007): Microsatellite instability in endometrioid type endometrial adenocarcinoma is associated with poor prognostic indicators. *The American journal of surgical pathology* 31 (6), 846–853.

ASTEC/EN.5 Study Group (2009): Adjuvant external beam radiotherapy in the treatment of endometrial cancer (MRC ASTEC and NCIC CTG EN.5 randomised trials). *The Lancet* 373 (9658), 137–146.

Banno, K.; Yanokura, M.; Iida, M.; Masuda, K.; Aoki, D. (2014): Carcinogenic mechanisms of endometrial cancer. *The journal of obstetrics and gynaecology research* 40 (8), 1957–1967.

Barry, J. A.; Azizia, M. M.; Hardiman, P. J. (2014): Risk of endometrial, ovarian and breast cancer in women with polycystic ovary syndrome. *Human reproduction update* 20 (5), 748–758.

Basil, J. B.; Goodfellow, P. J.; Rader, J. S.; Mutch, D. G.; Herzog, T. J. (2000): Clinical significance of microsatellite instability in endometrial carcinoma. *Cancer* 89 (8), 1758–1764.

Behjati, S.; Tarpey, P. S. (2013): What is next generation sequencing? *Archives of disease in childhood. Education and practice edition* 98 (6), 236–238.

Beral, V.; Bull, D.; Reeves, G. (2005): Endometrial cancer and hormone-replacement therapy in the Million Women Study. *Lancet (London, England)* 365 (9470), 1543–1551.

Bhattacharya, A.; Bense, R. D.; Urzúa-Traslaviña, C. G.; Vries, E. G. E. de; van Vugt, M. A. T. M.; Fehrmann, R. S. N. (2020): Transcriptional effects of copy number alterations in a large set of human cancers. *Nature communications* 11 (1), 715.

Bianchini, F.; Kaaks, R.; Vainio, H. (2002): Overweight, obesity, and cancer risk. *The Lancet. Oncology* 3 (9), 565–574.

Bishop, R. (2010): Applications of fluorescence in situ hybridization (FISH) in detecting genetic aberrations of medical significance. *Bioscience Horizons* 3 (1), 85–95.

Bokhman, J. V. (1983): Two pathogenetic types of endometrial carcinoma. *Gynecologic oncology* 15 (1), 10–17.

Bonneville, R.; Krook, M. A.; Kautto, E. A.; Miya, J.; Wing, M. R.; Chen, H.-Z. et al. (2017): Landscape of Microsatellite Instability Across 39 Cancer Types. *JCO precision oncology* 2017.

Chan, D. W.; Mak, C. S. L.; Leung, T. H. Y.; Chan, K. K. L.; Ngan, H. Y. S. (2012): Down-regulation of Sox7 is associated with aberrant activation of Wnt/b-catenin signaling in endometrial cancer. *Oncotarget* 3 (12), 1546–1556.

Ching, H. C.; Naidu, R.; Seong, M. K.; Har, Y. C.; Taib, N. A. M. (2011): Integrated analysis of copy number and loss of heterozygosity in primary breast carcinomas using high-density SNP array. *International journal of oncology* 39 (3), 621–633.

Church, D. N.; Briggs, S. E. W.; Palles, C.; Domingo, E.; Kearsey, S. J.; Grimes, J. M. et al. (2013): DNA polymerase ε and δ exonuclease domain mutations in endometrial cancer. *Human molecular genetics* 22 (14), 2820–2828.

Clarke, B. A.; Gilks, C. B. (2010): Endometrial carcinoma. Controversies in histopathological assessment of grade and tumour cell type. *Journal of clinical pathology* 63 (5), 410–415.

Colombo, N.; Creutzberg, C.; Amant, F.; Bosse, T.; González-Martín, A.; Ledermann, J. et al. (2016): ESMO-ESGO-ESTRO Consensus Conference on Endometrial Cancer. *International journal of gynecological cancer : official journal of the International Gynecological Cancer Society* 26 (1), 2–30.

Cosgrove, C. M.; Tritchler, D. L.; Cohn, D. E.; Mutch, D. G.; Rush, C. M.; Lankes, H. A. et al. (2018): An NRG Oncology/GOG study of molecular classification for risk prediction in endometrioid endometrial cancer. *Gynecologic oncology* 148 (1), 174–180.

Creasman, W. T.; Odicino, F.; Maisonneuve, P.; Beller, U.; Benedet, J. L.; Heintz, A. P. et al. (2003): Carcinoma of the corpus uteri. *International journal of gynaecology and obstetrics: the official organ of the International Federation of Gynaecology and Obstetrics* 83 Suppl 1, 79–118.

Croce, C. M. (2008): Oncogenes and cancer. *The New England journal of medicine* 358 (5), 502–511.

Davoli, T.; Xu, A. W.; Mengwasser, K. E.; Sack, L. M.; Yoon, J. C.; Park, P. J.; Elledge, S. J. (2013): Cumulative haploinsufficiency and triplosensitivity drive aneuploidy patterns and shape the cancer genome. *Cell* 155 (4), 948–962.

DeLair, D. F.; Burke, K. A.; Selenica, P.; Lim, R. S.; Scott, S. N.; Middha, S. et al. (2017): The genetic landscape of endometrial clear cell carcinomas. *The Journal of pathology* 243 (2), 230–241.

Denschlag, D.; Ackermann, S.; Battista, M. J.; Cremer, W.; Egerer, G.; Follmann, M. et al. (2019): Sarcoma of the Uterus. Guideline of the DGGG and OEGGG (S2k Level, AWMF Register Number 015/074, February 2019). *Geburtshilfe und Frauenheilkunde* 79 (10), 1043–1060.

Dizdar, O.; Arslan, C.; Altundag, K. (2015): Advances in PARP inhibitors for the treatment of breast cancer. *Expert opinion on pharmacotherapy* 16 (18), 2751–2758.

Edge, S. B.; Compton, C. C. (2010): The American Joint Committee on Cancer. The 7th edition of the AJCC cancer staging manual and the future of TNM. *Annals of surgical oncology* 17 (6), 1471–1474.

Erfani, M.; Hosseini, S. V.; Mokhtari, M.; Zamani, M.; Tahmasebi, K.; Alizadeh Naini, M. et al. (2020): Altered ARID1A expression in colorectal cancer. *BMC cancer* 20 (1), 350.

European Cancer Information System (2020): 2020 Cancer incidence and mortality in EU-27 countries. European Cancer Information System.

Friberg, E.; Mantzoros, C. S.; Wolk, A. (2007): Diabetes and risk of endometrial cancer. *Cancer epidemiology, biomarkers & prevention : a publication of the American Association for Cancer Research, cosponsored by the American Society of Preventive Oncology* 16 (2), 276–280.

Fung-Kee-Fung, M.; Dodge, J.; Elit, L.; Lukka, H.; Chambers, A.; Oliver, T. (2006): Follow-up after primary therapy for endometrial cancer. *Gynecologic oncology* 101 (3), 520–529.

Gavande, N. S.; VanderVere-Carozza, P. S.; Hinshaw, H. D.; Jalal, S. I.; Sears, C. R.; Pawelczak, K. S.; Turchi, J. J. (2016): DNA repair targeted therapy. *Pharmacology & therapeutics* 160, 65–83.

German Cancer Society, German Cancer Aid, AWMF (2018): Guideline on the Diagnosis, Treatment, and Follow-up of Patients with Endometrial cancer (032/034-OL).

Ghazali, W. A. H. W.; Jamil, S. A.; Sharin, I. A. (2019): Laparoscopic versus Laparotomy. Staging Surgery for Endometrial Cancer - Malaysia's Early Experience. *Gynecology and minimally invasive therapy* 8 (1), 25–29.

Girirajan, S.; Campbell, C. D.; Eichler, E. E. (2011): Human copy number variation and complex genetic disease. *Annual review of genetics* 45, 203–226.

Green, A. K.; Feinberg, J.; Makker, V. (2020): A Review of Immune Checkpoint Blockade Therapy in Endometrial Cancer. *American Society of Clinical Oncology educational book. American Society of Clinical Oncology. Annual Meeting* 40, 1–7.

Guan, B.; Mao, T.-L.; Panuganti, P. K.; Kuhn, E.; Kurman, R. J.; Maeda, D. et al. (2011): Mutation and loss of expression of ARID1A in uterine low-grade endometrioid carcinoma. *The American journal of surgical pathology* 35 (5), 625–632.

Haidopoulos, D.; Simou, M.; Akrivos, N.; Rodolakis, A.; Vlachos, G.; Fotiou, S. et al. (2010): Risk factors in women 40 years of age and younger with endometrial carcinoma. *Acta obstetricia et gynecologica Scandinavica* 89 (10), 1326–1330.

Hamilton, C. A.; Cheung, M. K.; Osann, K.; Chen, L.; Teng, N. N.; Longacre, T. A. et al. (2006): Uterine papillary serous and clear cell carcinomas predict for poorer survival compared to grade 3 endometrioid corpus cancers. *British journal of cancer* 94 (5), 642–646.

Hayes, M. P.; Wang, H.; Espinal-Witter, R.; Douglas, W.; Solomon, G. J.; Baker, S. J.; Ellenson, L. H. (2006): PIK3CA and PTEN mutations in uterine endometrioid carcinoma and complex atypical hyperplasia. *Clinical cancer research : an official journal of the American Association for Cancer Research* 12 (20 Pt 1), 5932–5935.

Hirasawa, A.; Aoki, D.; Inoue, J.; Imoto, I.; Susumu, N.; Sugano, K. et al. (2003): Unfavorable prognostic factors associated with high frequency of microsatellite instability and comparative genomic hybridization analysis in endometrial cancer. *Clinical cancer research : an official journal of the American Association for Cancer Research* 9 (15), 5675–5682.

Hong, B.; Le Gallo, M.; Bell, D. W. (2015): The mutational landscape of endometrial cancer. *Current opinion in genetics & development* 30, 25–31.

Howitt, B. E.; Shukla, S. A.; Sholl, L. M.; Ritterhouse, L. L.; Watkins, J. C.; Rodig, S. et al. (2015): Association of Polymerase e-Mutated and Microsatellite-Instable Endometrial Cancers With Neoantigen Load, Number of Tumor-Infiltrating Lymphocytes, and Expression of PD-1 and PD-L1. *JAMA oncology* 1 (9), 1319–1323.

Im Barth, A.; Näthke, I. S.; Nelson, W. J. (1997): Cadherins, catenins and APC protein. Interplay between cytoskeletal complexes and signaling pathways. *Current Opinion in Cell Biology* 9 (5), 683–690.

Inomata, M.; Ochiai, A.; Akimoto, S.; Kitano, S.; Hirohashi, S. (1996): Alteration of beta-catenin expression in colonic epithelial cells of familial adenomatous polyposis patients. *Cancer research* 56 (9), 2213–2217.

Janku, F.; Wheler, J. J.; Westin, S. N.; Moulder, S. L.; Naing, A.; Tsimberidou, A. M. et al. (2012): PI3K/AKT/mTOR inhibitors in patients with breast and gynecologic malignancies harboring PIK3CA mutations. *Journal of clinical oncology : official journal of the American Society of Clinical Oncology* 30 (8), 777–782.

Jeske, Y. W.; Ali, S.; Byron, S. A.; Gao, F.; Mannel, R. S.; Ghebre, R. G. et al. (2017): FGFR2 mutations are associated with poor outcomes in endometrioid endometrial cancer. *Gynecologic oncology* 145 (2), 366–373.

Jones, M. E.; van Leeuwen, F. E.; Hoogendoorn, W. E.; Mourits, M. J.; Hollema, H.; van Boven, H. et al. (2012): Endometrial cancer survival after breast cancer in relation to tamoxifen treatment. *Breast cancer research : BCR* 14 (3), R91.

Jonge, M. M. de; Ritterhouse, L. L.; Kroon, C. D. de; Vreeswijk, M. P. G.; Segal, J. P.; Puranik, R. et al. (2019): Germline BRCA-Associated Endometrial Carcinoma Is a Distinct Clinicopathologic Entity. *Clinical cancer research : an official journal of the American Association for Cancer Research* 25 (24), 7517–7526.

Jönsson, J.-M.; Bååth, M.; Björnheden, I.; Sahin, I. D.; Måsbäck, A.; Hedenfalk, I. (2021): Homologous Recombination Repair Mechanisms in Serous Endometrial Cancer. *Cancers* 13 (2).

Kanamori, Y.; Kigawa, J.; Itamochi, H.; Shimada, M.; Takahashi, M.; Kamazawa, S. et al. (2001): Correlation between loss of PTEN expression and Akt phosphorylation in endometrial carcinoma. *Clinical cancer research : an official journal of the American Association for Cancer Research* 7 (4), 892–895.

Kandoth, C.; Schultz, N.; Cherniack, A. D.; Akbani, R.; Liu, Y.; Shen, H. et al. (2013): Integrated genomic characterization of endometrial carcinoma. *Nature* 497 (7447), 67–73.

Kanopiene, D.; Vidugiriene, J.; Valuckas, K. P.; Smailyte, G.; Uleckiene, S.; Bacher, J. (2015): Endometrial cancer and microsatellite instability status. *Open medicine (Warsaw, Poland)* 10 (1), 70–76.

Khalique, S.; Naidoo, K.; Attygalle, A. D.; Kriplani, D.; Daley, F.; Lowe, A. et al. (2018): Optimised ARID1A immunohistochemistry is an accurate predictor of ARID1A mutational status in gynaecological cancers. *The journal of pathology. Clinical research* 4 (3), 154–166.

Kim, T.-M.; Laird, P. W.; Park, P. J. (2013): The landscape of microsatellite instability in colorectal and endometrial cancer genomes. *Cell* 155 (4), 858–868.

Konecny, G. E.; Finkler, N.; Garcia, A. A.; Lorusso, D.; Lee, P. S.; Rocconi, R. P. et al. (2015): Second-line dovitinib (TKI258) in patients with FGFR2-mutated or FGFR2-non-mutated advanced or metastatic endometrial cancer. *The Lancet Oncology* 16 (6), 686–694.

Kuhn, E.; Wu, R.-C.; Guan, B.; Wu, G.; Zhang, J.; Wang, Y. et al. (2012): Identification of molecular pathway aberrations in uterine serous carcinoma by genome-wide analyses. *Journal of the National Cancer Institute* 104 (19), 1503–1513.

Kurnit, K. C.; Kim, G. N.; Fellman, B. M.; Urbauer, D. L.; Mills, G. B.; Zhang, W.; Broaddus, R. R. (2017): CTNNB1 (beta-catenin) mutation identifies low grade, early stage endometrial cancer patients at

increased risk of recurrence. *Modern pathology : an official journal of the United States and Canadian Academy of Pathology, Inc* 30 (7), 1032–1041.

Lax, S. F.; Kendall, B.; Tashiro, H.; Slebos, R. J.; Hedrick, L. (2000): The frequency of p53, K-ras mutations, and microsatellite instability differs in uterine endometrioid and serous carcinoma. *Cancer* 88 (4), 814–824.

Le, D. T.; Durham, J. N.; Smith, K. N.; Wang, H.; Bartlett, B. R.; Aulakh, L. K. et al. (2017): Mismatch repair deficiency predicts response of solid tumors to PD-1 blockade. *Science (New York, N.Y.)* 357 (6349), 409–413.

Liang, H.; Cheung, L. W. T.; Li, J.; Ju, Z.; Yu, S.; Stemke-Hale, K. et al. (2012): Whole-exome sequencing combined with functional genomics reveals novel candidate driver cancer genes in endometrial cancer. *Genome research* 22 (11), 2120–2129.

Liu, L.; Jiang, H.; Wang, X.; Wang, X.; Zou, L. (2020): STYX/FBXW7 axis participates in the development of endometrial cancer cell via Notch-mTOR signaling pathway. *Bioscience reports* 40 (4).

Liu, Y.; Patel, L.; Mills, G. B.; Lu, K. H.; Sood, A. K.; Ding, L. et al. (2014): Clinical significance of CTNNB1 mutation and Wnt pathway activation in endometrioid endometrial carcinoma. *Journal of the National Cancer Institute* 106 (9).

López-Reig, R.; Fernández-Serra, A.; Romero, I.; Zorrero, C.; Illueca, C.; García-Casado, Z. et al. (2019): Prognostic classification of endometrial cancer using a molecular approach based on a twelve-gene NGS panel. *Scientific reports* 9 (1), 18093.

Lucito, R.; Healy, J.; Alexander, J.; Reiner, A.; Esposito, D.; Chi, M. et al. (2003): Representational oligonucleotide microarray analysis. *Genome research* 13 (10), 2291–2305.

Machin, P.; Catasus, L.; Pons, C.; Muñoz, J.; Matias-Guiu, X.; Prat, J. (2002): CTNNB1 mutations and beta-catenin expression in endometrial carcinomas. *Human pathology* 33 (2), 206–212.

Marra, G.; Boland, C. R. (1995): Hereditary nonpolyposis colorectal cancer. *Journal of the National Cancer Institute* 87 (15), 1114–1125.

McConechy, M. K.; Ding, J.; Cheang, M. C.; Wiegand, K.; Senz, J.; Tone, A. et al. (2012): Use of mutation profiles to refine the classification of endometrial carcinomas. *The Journal of pathology* 228 (1), 20–30.

McConechy, M. K.; Talhouk, A.; Leung, S.; Chiu, D.; Yang, W.; Senz, J. et al. (2016): Endometrial Carcinomas with POLE Exonuclease Domain Mutations Have a Favorable Prognosis. *Clinical cancer research : an official journal of the American Association for Cancer Research* 22 (12), 2865–2873.

Mehnert (2020): Pembrolizumab in Treating Participants With Metastatic, Recurrent or Locally Advanced Cancer and Genomic Instability. ClinicalTrials.gov Identifier: NCT03428802. With assistance of National Cancer Institute (NCI). Edited by Eugenia Girda, MD, Rutgers Cancer Institute of New Jersey. The State University of New Jersey. Available online at www.clinicaltrials.go, updated on 11/6/2020, checked on 12/25/2020.

Mehnert, J. M.; Panda, A.; Zhong, H.; Hirshfield, K.; Damare, S.; Lane, K. et al. (2016): Immune activation and response to pembrolizumab in POLE-mutant endometrial cancer. *The Journal of clinical investigation* 126 (6), 2334–2340.

Miyake, T.; Yoshino, K.; Enomoto, T.; Takata, T.; Ugaki, H.; Kim, A. et al. (2008): PIK3CA gene mutations and amplifications in uterine cancers, identified by methods that avoid confounding by PIK3CA pseudogene sequences. *Cancer letters* 261 (1), 120–126.

Moreno-Bueno, G.; Hardisson, D.; Sánchez, C.; Sarrió, D.; Cassia, R.; García-Rostán, G. et al. (2002): Abnormalities of the APC/beta-catenin pathway in endometrial cancer. *Oncogene* 21 (52), 7981–7990.

Morice, P.; Leary, A.; Creutzberg, C.; Abu-Rustum, N.; Darai, E. (2016): Endometrial cancer. *The Lancet* 387 (10023), 1094–1108.

Murali, R.; Soslow, R. A.; Weigelt, B. (2014): Classification of endometrial carcinoma. More than two types. *The Lancet Oncology* 15 (7), e268-e278.

Musacchio, L.; Caruso, G.; Pisano, C.; Cecere, S. C.; Di Napoli, M.; Attademo, L. et al. (2020): PARP Inhibitors in Endometrial Cancer. *Cancer management and research* 12, 6123–6135.

Myers, A.; Barry, W. T.; Hirsch, M. S.; Matulonis, U.; Lee, L. (2014): β-Catenin mutations in recurrent FIGO IA grade I endometrioid endometrial cancers. *Gynecologic oncology* 134 (2), 426–427.

National Cancer Institute: Cancer Stat Facts: Uterine Cancer. National Cancer Institute.

NCT03981796: A Study to Evaluate Dostarlimab Plus Carboplatin-paclitaxel Versus Placebo Plus Carboplatin-paclitaxel in Participants With Recurrent or Primary Advanced Endometrial Cancer (RUBY). With assistance of European Network of Gynaecological Oncological Trial Groups (ENGOT). Tesaro, Inc. Available online at https://clinicaltrials.gov/ct2/show/NCT03981796.

Nei, H.; Saito, T.; Yamasaki, H.; Mizumoto, H.; Ito, E.; Kudo, R. (1999): Nuclear localization of β-catenin in normal and carcinogenic endometrium. *Mol. Carcinog.* 25 (3), 207–218.

Okuda, T.; Sekizawa, A.; Purwosunu, Y.; Nagatsuka, M.; Morioka, M.; Hayashi, M.; Okai, T. (2010): Genetics of endometrial cancers. *Obstetrics and gynecology international* 2010, 984013.

O'Mara, T. A.; Glubb, D. M.; Kho, P. F.; Thompson, D. J.; Spurdle, A. B. (2019): Genome-Wide Association Studies of Endometrial Cancer. *Cancer epidemiology, biomarkers & prevention : a publication of the American Association for Cancer Research, cosponsored by the American Society of Preventive Oncology* 28 (7), 1095–1102.

Park, J.-Y.; Kim, D.-Y.; Kim, T.-J.; Kim, J. W.; Kim, J.-H.; Kim, Y.-M. et al. (2013): Hormonal therapy for women with stage IA endometrial cancer of all grades. *Obstetrics and gynecology* 122 (1), 7–14.

Robert-Koch-Institut: Gesellschaft der epidemiologischen Krebsregister in Deutschland e.V. RKI. Available online at http://edoc.rki.de/176904/6012.

Ryland, G. L.; Doyle, M. A.; Goode, D.; Boyle, S. E.; Choong, D. Y. H.; Rowley, S. M. et al. (2015): Loss of heterozygosity. *BMC medical genomics* 8, 45.

Sailo, B. L.; Banik, K.; Girisa, S.; Bordoloi, D.; Fan, L.; Halim, C. E. et al. (2019): FBXW7 in Cancer. *Cancers* 11 (2).

Salehi, S.; Åvall-Lundqvist, E.; Legerstam, B.; Carlson, J. W.; Falconer, H. (2017): Robot-assisted laparoscopy versus laparotomy for infrarenal paraaortic lymphadenectomy in women with high-risk endometrial cancer. *European journal of cancer (Oxford, England : 1990)* 79, 81–89.

Segditsas, S.; Rowan, A. J.; Howarth, K.; Jones, A.; Leedham, S.; Wright, N. A. et al. (2009): APC and the three-hit hypothesis. *Oncogene* 28 (1), 146–155.

Shao, X.; Lv, N.; Liao, J.; Long, J.; Xue, R.; Ai, N. et al. (2019): Copy number variation is highly correlated with differential gene expression. *BMC medical genetics* 20 (1), 175.

Shao, Y.; Cheng, S.; Hou, J.; Zuo, Y.; Zheng, W.; Xia, M.; Mu, N. (2016): Insulin is an important risk factor of endometrial cancer among premenopausal women. *Tumour biology : the journal of the International Society for Oncodevelopmental Biology and Medicine* 37 (4), 4721–4726.

Shaw, E.; Farris, M.; McNeil, J.; Friedenreich, C. (2016): Obesity and Endometrial Cancer. *Recent results in cancer research. Fortschritte der Krebsforschung. Progres dans les recherches sur le cancer* 208, 107–136.

Sherman, M. E.; Devesa, S. S. (2003): Analysis of racial differences in incidence, survival, and mortality for malignant tumors of the uterine corpus. *Cancer* 98 (1), 176–186.

Sherwood, J. B.; Shivapurkar, N.; Lin, W. M.; Ashfaq, R.; Miller, D. S.; Gazdar, A. F.; Muller, C. Y. (2000): Chromosome 4 deletions are frequent in invasive cervical cancer and differ between histologic variants. *Gynecologic oncology* 79 (1), 90–96.

Shivapurkar, N.; Maitra, A.; Milchgrub, S.; Gazdar, A. F. (2001): Deletions of chromosome 4 occur early during the pathogenesis of colorectal carcinoma. *Human pathology* 32 (2), 169–177.

Shrivastav, M.; Haro, L. P. de; Nickoloff, J. A. (2008): Regulation of DNA double-strand break repair pathway choice. *Cell research* 18 (1), 134–147.

Siegel, R. L.; Miller, K. D.; Jemal, A. (2020): Cancer statistics, 2020. *CA: a cancer journal for clinicians* 70 (1), 7–30.

Sorbe, B.; Nordström, B.; Mäenpää, J.; Kuhelj, J.; Kuhelj, D.; Okkan, S. et al. (2009): Intravaginal brachytherapy in FIGO stage I low-risk endometrial cancer. *International journal of gynecological cancer : official journal of the International Gynecological Cancer Society* 19 (5), 873–878.

Stelloo, E.; Bosse, T.; Nout, R. A.; MacKay, H. J.; Church, D. N.; Nijman, H. W. et al. (2015): Refining prognosis and identifying targetable pathways for high-risk endometrial cancer; a TransPORTEC initiative. *Modern pathology : an official journal of the United States and Canadian Academy of Pathology, Inc* 28 (6), 836–844.

Stelloo, E.; Nout, R. A.; Osse, E. M.; Jürgenliemk-Schulz, I. J.; Jobsen, J. J.; Lutgens, L. C. et al. (2016): Improved Risk Assessment by Integrating Molecular and Clinicopathological Factors in Early-stage Endometrial Cancer-Combined Analysis of the PORTEC Cohorts. *Clinical cancer research : an official journal of the American Association for Cancer Research* 22 (16), 4215–4224.

Talhouk, A.; McConechy, M. K.; Leung, S.; Li-Chang, H. H.; Kwon, J. S.; Melnyk, N. et al. (2015): A clinically applicable molecular-based classification for endometrial cancers. *British journal of cancer* 113 (2), 299–310.

Talhouk, A.; McConechy, M. K.; Leung, S.; Yang, W.; Lum, A.; Senz, J. et al. (2017): Confirmation of ProMisE. *Cancer* 123 (5), 802–813.

Tavassoli, Fattaneh A.; Devilee, Peter (2003): Pathology and genetics of tumours of the breast and female genital organs. Lyon: International Agency for Research on Cancer; Oxford : Oxford University Press [distributor] (World Health Organisation classification of tumours).

TCGA Pan Cancer Atlas: TCGA PanCancer Atlas Studies (https://www.cbioportal.org/). With assistance of PanCanAtlas Publications. Edited by cbioportal.org. Available online at https://www.cbioportal.org/results/cancerTypesSummary?case_set_id=all&gene_list=APC&cancer_study_list=5c8a7d55e4b046111fee2296.

Thiagalingam, S.; Foy, R. L.; Cheng, K.-h.; Lee, H. J.; Thiagalingam, A.; Ponte, J. F. (2002): Loss of heterozygosity as a predictor to map tumor suppressor genes in cancer. *Current opinion in oncology* 14 (1), 65–72.

Turner, N.; Tutt, A.; Ashworth, A. (2004): Hallmarks of 'BRCAness' in sporadic cancers. *Nature reviews. Cancer* 4 (10), 814–819.

Urick, M. E.; Bell, D. W. (2019): Clinical actionability of molecular targets in endometrial cancer. *Nature reviews. Cancer* 19 (9), 510–521.

van den Heerik, A. S. V. M.; Horeweg, N.; Boer, S. M. de; Bosse, T.; Creutzberg, C. L. (2020a): Adjuvant therapy for endometrial cancer in the era of molecular classification. *International journal of gynecological cancer : official journal of the International Gynecological Cancer Society*.

van den Heerik, A. S. V. M.; Horeweg, N.; Nout, R. A.; Lutgens, L. C. H. W.; van der Steen-Banasik, E. M.; Westerveld, G. H. et al. (2020b): PORTEC-4a. *International journal of gynecological cancer : official journal of the International Gynecological Cancer Society* 30 (12), 2002–2007.

van Loo, P.; Nilsen, G.; Nordgard, S. H.; Vollan, H. K. M.; Børresen-Dale, A.-L.; Kristensen, V. N.; Lingjærde, O. C. (2012): Analyzing cancer samples with SNP arrays. *Methods in molecular biology (Clifton, N.J.)* 802, 57–72.

Venesio, T.; Balsamo, A.; Rondo-Spaudo, M.; Varesco, L.; Risio, M.; Ranzani, G. N. (2003): APC haploinsufficiency, but not CTNNB1 or CDH1 gene mutations, accounts for a fraction of familial adenomatous polyposis patients without APC truncating mutations. *Laboratory investigation; a journal of technical methods and pathology* 83 (12), 1859–1866.

Wang, J. J.; Peng, K. Y.; Wu, V. C.; Tseng, F. Y.; Wu, K. D. (2017): CTNNB1 Mutation in Aldosterone Producing Adenoma. *Endocrinology and metabolism (Seoul, Korea)* 32 (3), 332–338.

Watkins, J. A.; Irshad, S.; Grigoriadis, A.; Tutt, A. N. J. (2014): Genomic scars as biomarkers of homologous recombination deficiency and drug response in breast and ovarian cancers. *Breast cancer research : BCR* 16 (3), 211.

Weimer, J.; Nusilati, A.; Tiemann, K.; Stope, M. B.; Mustea, A.; Karow, D. et al. (2018): Array based Copy number variations (aCNV) are able to differ classes in endometrial carcinoma. In. Abstracts of the 10th Scientific Symposium of the Comission for Translational Research of the Working group for Gynecologic Oncology AGO e.V. Düsseldorf, 7/9/2018 - 8/9/2018: Georg Thieme Verlag KG (Geburtshilfe und Frauenheilkunde).

Wilczyński, M.; Danielska, J.; Wilczyński, J. (2016): An update of the classical Bokhman's dualistic model of endometrial cancer. *Przeglad menopauzalny = Menopause review* 15 (2), 63–68.

Win, A. K.; Young, J. P.; Lindor, N. M.; Tucker, K. M.; Ahnen, D. J.; Young, G. P. et al. (2012): Colorectal and other cancer risks for carriers and noncarriers from families with a DNA mismatch repair gene mutation. *Journal of clinical oncology : official journal of the American Society of Clinical Oncology* 30 (9), 958–964.

Yeh, C.-H.; Bellon, M.; Nicot, C. (2018): FBXW7. *Molecular cancer* 17 (1), 115.

Zhang, L.; Poh, C. F.; Williams, M.; Laronde, D. M.; Berean, K.; Gardner, P. J. et al. (2012a): Loss of heterozygosity (LOH) profiles--validated risk predictors for progression to oral cancer. *Cancer prevention research (Philadelphia, Pa.)* 5 (9), 1081–1089.

Zhang, Z.; Zhou, D.; Lai, Y.; Liu, Y.; Tao, X.; Wang, Q. et al. (2012b): Estrogen induces endometrial cancer cell proliferation and invasion by regulating the fat mass and obesity-associated gene via PI3K/AKT and MAPK signaling pathways. *Cancer letters* 319 (1), 89–97.

Danksagung

Ich möchte nun die Möglichkeiten nutzen, um den Menschen zu danken, die diese Arbeit möglich gemacht haben. An erster Stelle möchte ich mich ganz herzlich bei meinem Doktorvater Prof. Dr. Norbert Arnold für die freundliche Aufnahme in das onkologische Labor der Frauenklinik UKSH Kiel bedanken. Außerdem möchte ich mich für die Überlassung des interessanten Promotionsthemas und die stete Diskussionsbereitschaft bedanken. Ein weiterer großer Dank geht an Dr. Jörg Weimer für die tolle Betreuung und die immer offene Tür über die komplette Promotionszeit. Danke für die vielen wertvollen Diskussionen, die ganzen Hilfestellungen und deine Geduld. Prof. Dr. Dirk Bauerschlag möchte ich für die stetige Unterstützung und seine Motivation danken.

Ein besonderes Dankeschön geht an Doris Karow und Sigrid Hamann für die angenehme Zeit im Büro, die zahlreiche Unterstützung im Labor und die vielen Ratschläge. Auch bei Dr. Nina Hedemann möchte ich mich für die stetige gute Laune und Unterstützung bedanken. Bei dem gesamten Laborteam möchte ich mich dafür bedanken, dass ich so herzlich ins Team aufgenommen wurde, ich mich immer willkommen und wohl gefühlt habe.

Aus Kollegen sind gute Freunde geworden. Für die zahlreichen schönen Momente auch außerhalb des Labors möchte ich Dr. Inken Flörkemeier, Dr. Sabrina Farrokh and Catharina Verkooyen danken.

Für das Korrekturlesen dieser Arbeit danke ich insbesondere Dr. Jörg Weimer und Dr. Inken Flörkemeier.

Abschließend möchte ich mich noch bei meinen Eltern, meiner Schwester und meinem Mann bedanken. Danke für eure Unterstützung, euer Verständnis und euren Rückhalt. Ohne euer offenes Ohr zu jeder Zeit bei kleinen und großen Schwierigkeiten, hätte ich dies nicht erreicht.